Copy 6
RM A52F27

NACA

NACA RM A52F27

RESEARCH MEMORANDUM

INVESTIGATION OF DRAG AND PRESSURE RECOVERY OF A SCOOP INLET IN THE TRANSONIC SPEED RANGE

By James Selna, Loren G. Bright, and Bernard A. Schlaff

Ames Aeronautical Laboratory
Moffett Field, Calif.

NATIONAL ADVISORY COMMITTEE FOR AERONAUTICS

WASHINGTON
December 15, 1952

NACA RM A52F27

NATIONAL ADVISORY COMMITTEE FOR AERONAUTICS

RESEARCH MEMORANDUM

INVESTIGATION OF DRAG AND PRESSURE RECOVERY OF A SCOOP INLET IN THE TRANSONIC SPEED RANGE

By James Selna, Loren G. Bright,
and Bernard A. Schlaff

SUMMARY

The drag and pressure recovery of a scoop-inlet model have been investigated at transonic speeds by the free-fall testing technique over a Mach number range from about 0.8 to 1.12. Tests were conducted at zero angle of attack, using both rounded and sharp lips at mass-flow ratios from about 0.6 to 0.9.

The results indicate that the Mach number of drag divergence of the scoop-inlet model was about the same as that of the basic model without inlets which was tested previously. Rounding the inlet lips caused an increase in external drag coefficient (based on the maximum cross-sectional area of the model) of about 0.01 for the range of the tests. This difference, when expressed in terms of a typical current airplane configuration with a ratio of maximum fuselage cross-sectional area to wing area of 0.06, would result in a small increase in airplane total drag coefficient of about 0.0006.

A comparison of the performance of the scoop-inlet model of this report with similar results previously obtained for an NACA submerged inlet and an NACA 1-series nose inlet is presented.

INTRODUCTION

In order to evaluate the most efficient type of air inlet for use in aircraft air-induction systems, comparable data are required on the aerodynamic characteristics of various types of inlets.

The NACA has undertaken an investigation employing large-scale free-fall models to provide drag and pressure-recovery information on several

types of inlets in the transonic speed range. Comparable data on an NACA 1-series nose-inlet model and an NACA submerged-inlet model were provided in references 1 and 2.

The purpose of the present investigation was to obtain drag and pressure-recovery characteristics of a scoop-inlet model in the transonic speed range, and to compare these characteristics with those for the nose-inlet and submerged-inlet models previously tested.

The investigation included tests of the scoop inlet without boundary-layer control ducting and with a rounded lip and with a sharp lip. The tests were conducted over a mass-flow-ratio range of about 0.6 to 0.9 for a Mach number range of 0.8 to about 1.12. The investigation was conducted using large scale, free-fall recoverable models.

SYMBOLS

A	cross-sectional area of one duct, square feet
C_{D_T}	total drag coefficient $\left(\frac{D_T}{q_o S}\right)$
C_{D_I}	internal drag coefficient $\left(\frac{D_I}{q_o S}\right)$
C_{D_E}	external drag coefficient $\left(C_{D_T} - C_{D_I}\right)$
C_{D_a}	inlet incremental drag coefficient $\left(\frac{D_a}{q_o S}\right)$
C_{D_A}	additive drag coefficient $\left(\frac{D_A}{q_o S}\right)$
D_T	total drag, pounds
D_I	internal drag, pounds
D_E	external drag $\left(D_T - D_I\right)$, pounds
D_a	inlet incremental drag, pounds
D_A	additive drag, pounds
d	duct depth at duct entrance, inches

H	total pressure, pounds per square foot
$\frac{H-p_o}{H_o-p_o}$	ram-recovery ratio, dimensionless
M	Mach number, dimensionless
m	mass flow, slugs per second
$\frac{m_1}{m_o}$	mass-flow ratio $\left(\frac{\rho_1 A_1 V_1}{\rho_o A_1 V_o}\right)$, dimensionless
p	static pressure, pounds per square foot
q	dynamic pressure $\left(\frac{1}{2}\rho V^2\right)$, pounds per square foot
S	cross-sectional area of model at maximum diameter, square feet
V	velocity, feet per second
ρ	mass density of air, slugs per cubic foot

Subscripts

o	free stream
1	duct entrance (station 62)
2	station 86.5
3	station 97
4	station 134
a,b,c,d	separate measurements at a given station
s	surface

TEST TECHNIQUE AND MODEL

The present investigation was conducted employing the recoverable free-fall-model technique described in reference 1. In this technique, the model is released from a carrier airplane at about 40,000 feet

pressure altitude and allowed to accelerate in free fall to an altitude of approximately 18,000 feet where recovery is initiated. The Mach number attained at this altitude is about 1.12.

The scoop-inlet model is shown in figure 1. The inlets were installed in the same basic body (fig. 2) employed in previous tests of a submerged inlet and a nose inlet (references 1 and 2). The model was 211 inches in length (exclusive of nose-boom length) with a fineness ratio of 12.4 and weighed about 1100 pounds. The screws used to attach the external skins to the model were inserted flush to the skin, but were not filled with any smoothing compound. The hangers, used to attach the model to the carrier airplane, were retracted into the model, flush with the skin, when the model was released. The airspeed head used on the model is described in reference 2. The fins on the model were oriented for 0° incidence on all tests.

The details of the scoop-inlet model, including the ducting and inlet details, are shown in figure 3. The inlet was designed for a relatively low aspect ratio, about 1.65, in order to minimize the amount of boundary-layer air flowing into it. The two lip shapes employed in the tests are shown in figure 3(b). The shape of the rounded lip is similar to that of lip E of reference 3. The leading edge of the sharp lip had a wedge angle of about 8.5°.

INSTRUMENTATION AND TEST

The instruments employed in the model and the carrier airplane, their purpose, ranges, and estimated accuracy are described in reference 1.

The instruments installed in the model consisted of an airspeed and altitude recorder, a sensitive accelerometer for measuring total drag, and recording manometers to measure various pressures. All instruments were compensated for the temperatures experienced within the heated interior of the model.

The locations of the pressure tubes and orifices in the model ducting are shown in figure 3(c). The pressure rakes were installed at station 86.5 to evaluate ram-recovery ratio and at station 134 to obtain the pressure measurements required in evaluating internal drag. Various nozzles were installed in the ducting at station 97 to control the internal flow. These nozzles, except in the case of maximum-flow rate, were employed as sonic throats to measure the internal-flow rate. Orifices were installed along the surface of the model, forward of the duct floor center line of one inlet, along one inlet lip, and behind the lip to obtain pressure-distribution data. These orifice locations are shown in figure 3(d).

[redacted]

The pressure measuring system was designed to render any effects of lag negligible. For longer lines, such as airspeed head lines, the tubing employed was 3/16-inch inside diameter. For shorter lines, 1/8-inch inside-diameter tubing was used.

Instruments were installed in a temperature controlled compartment of the carrier airplane to record atmospheric data at 1000-foot intervals during the ascent of the airplane and to record model release conditions. The airplane was oriented in level flight at about 40,000-feet pressure altitude for the drop run. After release, the model accelerated in free fall up to a Mach number of about 1.12. Typical Reynolds number and Mach number variation during the free fall are given in figure 4.

The tests included drops at zero angle of attack of the rounded-lip scoop-inlet model employing throat-to-inlet-area ratios of 0.683, 0.777, 0.889, and 1.0 (mass-flow ratios of about 0.6, 0.7, 0.8, and 0.9) and drops of the sharp-lip scoop-inlet model employing throat-to-inlet-area ratios of 0.777, 0.889, and 1.0 (mass-flow ratios of about 0.7, 0.8, and 0.9).

REDUCTION OF DATA

The static pressure error coefficients for the airspeed head, which had been evaluated in previous tests (fig. 9 of reference 2), were employed in the calculation of free-stream Mach number. Internal drag was calculated as described in reference 1. The mass-flow ratio, when sonic throats were employed, was evaluated as described in reference 1. For a throat-to-inlet-area ratio of 1 in which flow through the throat was not sonic, the mass-flow ratio was calculated from total and static pressure measurements at the exit (station 134). In evaluating the ram-recovery ratios at station 86.5, an arithmetic average of the total pressure measurements was employed. The ram-recovery ratios, although evaluated for station 86.5, may also be considered as the pressure recovery at the inlet because of the high internal-duct efficiency measured in ground tests.

For the scoop-inlet model with sharp lips at a sonic-throat-to-inlet-area ratio of 0.889, no pressure data were obtained. In order to evaluate external drag, the internal-drag coefficients were assumed to be the same as those obtained with the rounded lip with the same sonic-throat-to-inlet-area ratio. A comparison of the internal-drag coefficients for the sharp and rounded lip tests at sonic-throat-to-inlet-area ratios of 0.777 and 1.00 indicated that this assumption was valid.

ACCURACY OF RESULTS

The accuracy of the test method was evaluated from the scatter of the experimental data (reference 2). The following is a tabulation of the maximum errors in free-stream Mach number, mass-flow ratio, and external drag:

M_o	± 0.02 at a Mach number of 0.75 ± 0.01 at Mach number above 0.85
m_1/m_o	± 0.01
C_{D_E}	± 0.01 below a Mach number of 1 ± 0.005 above a Mach number of 1

RESULTS

The variation of drag coefficients, ram recovery, and mass-flow ratio with free-stream Mach number for the scoop-inlet model with rounded and sharp lips is shown in figures 5 and 6.

The local Mach number distribution along the surface of the model ahead of the scoop inlet with a rounded lip is shown in figure 7 for mass-flow ratios of about 0.6 and 0.9. The pressure-coefficient distribution along the outside surface of the model behind the scoop inlet with rounded lip is shown in figure 8 for mass-flow ratios of about 0.6 and 0.9. The variation of the pressure coefficients at each orifice location on the rounded lip with free-stream Mach number is presented in figure 9 for a mass-flow ratio of about 0.9. The pressure-coefficient distribution along the center line of the model behind the scoop inlet with a sharp lip is given in figure 10 for mass-flow ratios of about 0.7 and 0.9. The variation of the pressure coefficients on the sharp lip with free-stream Mach number is shown in figure 11 at a mass-flow ratio of about 0.9.

The variation of the external-drag coefficient with mass-flow ratio at various Mach numbers for the scoop-inlet model with rounded and sharp lips is shown in figure 12. In figure 13 the data of figure 12 are compared with similar data from reference 2 for an NACA 1-series nose inlet and an NACA submerged inlet. The variation with free-stream Mach number of the external drag less the computed inlet incremental drag is presented in figure 14 for the scoop-inlet models and for the nose- and submerged-inlet models of reference 2. The external drag less additive drag for the nose-inlet model is also presented in figure 14.

[redacted]

The variation of the ram-recovery ratio with mass-flow ratio at several free-stream Mach numbers for the scoop-inlet models with rounded and sharp lips is shown in figure 15. These data are also compared with similar data from reference 2 for a submerged-inlet model.

DISCUSSION

Drag

A comparison of the drag data of figures 5 and 6 for the scoop-inlet model with similar data for the basic model without inlets, shown in figure 5(a), indicates that the Mach number of drag divergence of the scoop-inlet model was about the same as that of the basic model. The Mach number of drag divergence for the scoop-inlet model with rounded lips occurred at a free-stream Mach number considerably higher than that at which the local flow over the outside of the lip became supersonic. Figure 9 illustrates that the local flow along the rounded lip was supersonic at Mach numbers above about 0.70. Drag divergence (fig. 5) did not occur until a free-stream Mach number of well above 0.90 was reached.

Figure 12 illustrates that the external drag of the model with sharp lips was less than that of the rounded-lip model throughout the Mach number and mass-flow ranges of the tests. The difference in the drag coefficients, when based on the maximum cross-sectional area of the model, was about 0.01 for the range of the tests. This difference would amount to about 0.0006 when expressed in terms of the change in total drag of a typical current airplane configuration with a ratio of maximum fuselage cross-sectional area to wing area of 0.06. The increased drag effect of the rounded-lip inlet is to be expected at higher values of Mach number, but not at lower values. However, the external-drag data presented from previous tests (references 4, 5, and 6) of sharp- and rounded-lip-inlet installations, at a mass-flow ratio of about 0.8, substantiate the results of these tests. A comparison of the results of these references indicates that at Mach numbers of 0.25, 1.5, and 2.0 the external-drag coefficient for a rounded lip was greater than that for a sharp lip by about 0.003, 0.02, and 0.04, respectively, based on fuselage cross-sectional area. For the airplane configuration previously mentioned, the corresponding differences in airplane total-drag coefficient would be 0.0002, 0.0012, and 0.0024. At values of design Mach number below 1.5, therefore, the available test data for thin inlet lips indicate that the external drag difference between a round and a sharp lip is relatively small, and other factors such as ram recovery may be the governing consideration in selecting the lip shape. However, at higher values of design Mach number this drag difference may dictate use of a sharp-lip inlet.

[redacted]

The increase of external drag coefficient with increasing mass-flow ratio shown in parts (a), (b), and (c) of figures 12 and 13 is not consistent with previous investigations which show either a decrease in drag, or constant drag as in parts (d), (e), and (f) of figures 12 and 13. This apparent inconsistency is believed traceable to the fact that the inducted air for the test models of this investigation was discharged into the model boundary layer forward of the tail surfaces, thus influencing the drag of the model surface behind the exits and also the model tail. This peculiarity of the test models should have no effect, however, on the comparison of the external drags of the sharp- and round-lip inlets, provided the comparisons are made at the same mass-flow ratio.

A comparison of the external drag of the scoop-inlet model with similar data given in reference 2 for a submerged-inlet model and a nose-inlet model is given in figure 13. The submerged-inlet model had the highest external drag coefficient throughout the Mach number and mass-flow range of the tests. Subsonically, the scoop inlet with sharp lips had the least drag. Supersonically, the nose inlet had the lowest external drag at the lower mass-flow ratios, and about the same external drag as that of the scoop inlet with the sharp lip at the higher mass-flow ratios. The maximum difference in external drag due to the inlet employed, for the various inlets compared in figure 13, amounts to about 20 percent of the basic model drag at subsonic speeds, and about 10 percent of the basic model drag at supersonic speeds.

A further breakdown to show the drag of the external surfaces of the inlet models ($C_{D_E} - C_{D_a}$) is shown in figure 14. If ($C_{D_E} - C_{D_A}$) is considered for the nose-inlet model (this subtracts the drag of the nose boom which is quite large due to the adverse pressure gradient on the boom of this model, see reference 2) the external surface drag of the nose-inlet model is generally less than that of the other inlet models.

The outlet employed in the present tests was not of a conventional design; consequently, there is little significance to a comparison of the external drag coefficients of the inlet models with that of the basic model. However, since the same air-outlet configuration was employed for the tests of this report and also those reported in references 1 and 2, a comparison of the external drag coefficients for the nose inlet, submerged inlet, and scoop inlet with round and sharp lips is justified.

Ram-Recovery Ratios

The ram-recovery ratio for the scoop inlet with rounded lips (fig. 15) was practically the same at each Mach number. The total pressure losses due to shock losses ahead of the inlets would be slight

[redacted]

because of the low supersonic velocities that prevailed ahead of the inlet (fig. 7). The ram-recovery ratio increased with increasing mass-flow ratio, as would be expected since there is an improvement in the pressure gradient immediately ahead of the inlet with increasing mass-flow ratio, and hence a reduction in boundary-layer thickness. The pressure recovery would continue to increase with increasing mass-flow ratio until internal separation prevailed.

The ram-recovery ratio for the scoop inlet with sharp lips (fig. 15) was less than that for the inlet with rounded lips at all Mach numbers, the difference increasing with increasing Mach number.

The comparison of the ram recovery of the scoop inlet with that for the submerged inlet of reference 2 (fig. 15) indicates that the submerged inlet yielded the highest ram recovery at mass-flow ratios below 0.7 up to a free-stream Mach number of 1.05. For the range of comparable data, the scoop inlet with rounded lips yielded the highest ram-recovery ratios throughout the Mach number range at mass-flow ratios above 0.7 and at all mass-flow ratios above a Mach number of 1.05.

Lip Pressure Distributions

The lip pressure distributions (figs. 8, 9, 10, and 11) show the pressure changes on the lips and afterbodies of the models as affected by Mach number and mass-flow ratio.

The leading-edge suction on the outer surface of the rounded lip (fig. 8) decreased with increasing free-stream Mach number and increased with decreasing mass-flow ratio.

For the sharp lip (fig. 10) measurements were not made as close to the lip leading edge as they were for the rounded lip due to lack of space. The data available, however, as pointed out previously, indicate no significant separation. In fairing the curves through the data points in figure 10, the points at station 66.43 were neglected because their deviation from the curves established by the remaining points is believed to be caused by local surface conditions peculiar to the test model.

It is of interest to note (fig. 11) that the pressure measurements nearest the sharp-lip leading edge indicate that, at a mass-flow ratio of 0.9, the flow over the lip was subsonic up to the highest test Mach number. This is probably a result of the change in static pressure of the stream in flowing through the detached shock wave which would exist ahead of the lip.

[redacted]

CONCLUSIONS

The following conclusions are based on the results of an investigation of the drag and pressure recovery of a scoop-inlet model with rounded and sharp lips in the transonic speed range, and a comparison of these results with similar data for submerged- and nose-inlet models tested under identical conditions:

1. The Mach number of drag divergence of the scoop-inlet models was about the same as that of a basic model without inlets which was tested previously.

2. The external drag of the scoop-inlet model was less with sharp lips than with rounded lips. Other data, at subsonic as well as supersonic speeds, substantiate this result. However, the drag differences between the sharp and round lip measured in this investigation (at transonic speeds) were small when expressed in terms of the change in total drag of a typical current airplane configuration.

3. A comparison of the results for the scoop-inlet model with those previously obtained for a submerged- and a nose-inlet model indicated: (1) The external drag of the submerged inlet was higher than that for the other inlets tested; (2) at subsonic speeds the minimum external drag was achieved by the scoop inlet with sharp lips and, at supersonic speeds, by the scoop inlet with sharp lips and the nose inlet, both configurations having about the same external drag in this speed range; and (3) the ram-recovery ratio of the scoop inlet was superior to that of the submerged inlet at mass-flow ratios above 0.75.

Ames Aeronautical Laboratory
National Advisory Committee for Aeronautics
Moffett Field, California

REFERENCES

1. Selna, James: Preliminary Investigation of a Submerged Inlet and a Nose Inlet in the Transonic Flight Range With Free-Fall Models. NACA RM A51B14, 1951.

2. Selna, James, and Schlaff, Bernard A.: An Investigation of the Drag and Pressure Recovery of a Submerged Inlet and a Nose Inlet in the Transonic Flight Range With Free-Fall Models. NACA RM A51H20, 1951.

3. Watson, Earl C.: Some Low-Speed Characteristics of an Air-Induction System Having Scoop-Type Inlets With Provisions for Boundary-Layer Control. NACA RM A51F15, 1951.

4. Nichols, Mark R., and Pendley, Robert E.: Performance of Air Inlets at Transonic and Low Supersonic Speeds. NACA RM L52A07, 1952.

5. Holzhauser, Curt A.: The Effect of Entrance Mach Number and Lip Shape on the Subsonic Characteristics of a Scoop-Type Air-Induction System for a Supersonic Airplane. NACA RM A51J19a, 1951.

6. Weinstein, M. I.: Performance of Supersonic Scoop Inlets. NACA RM E52A22, 1952.

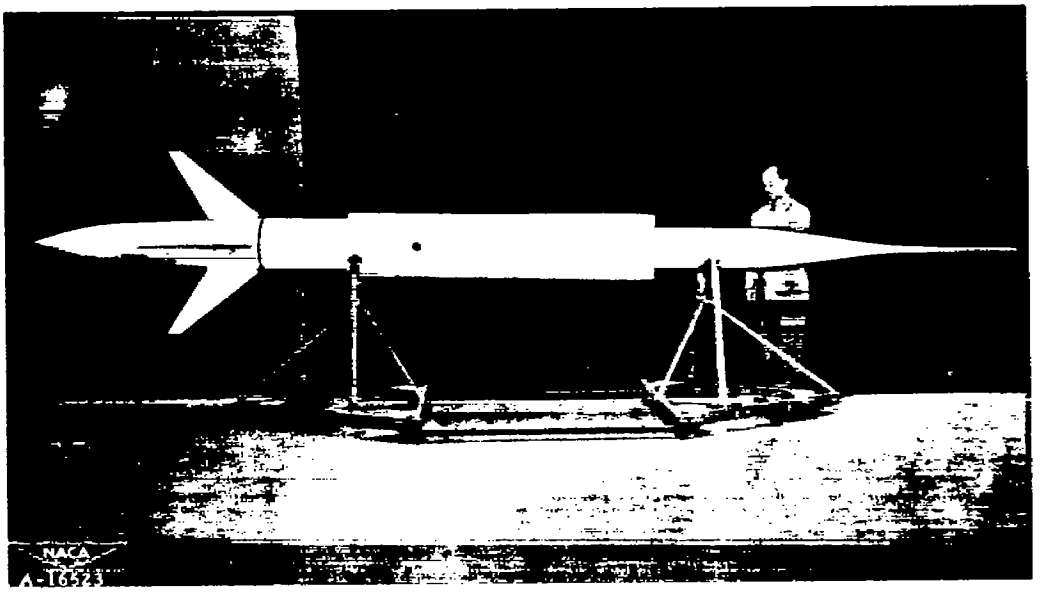

(a) Top view.

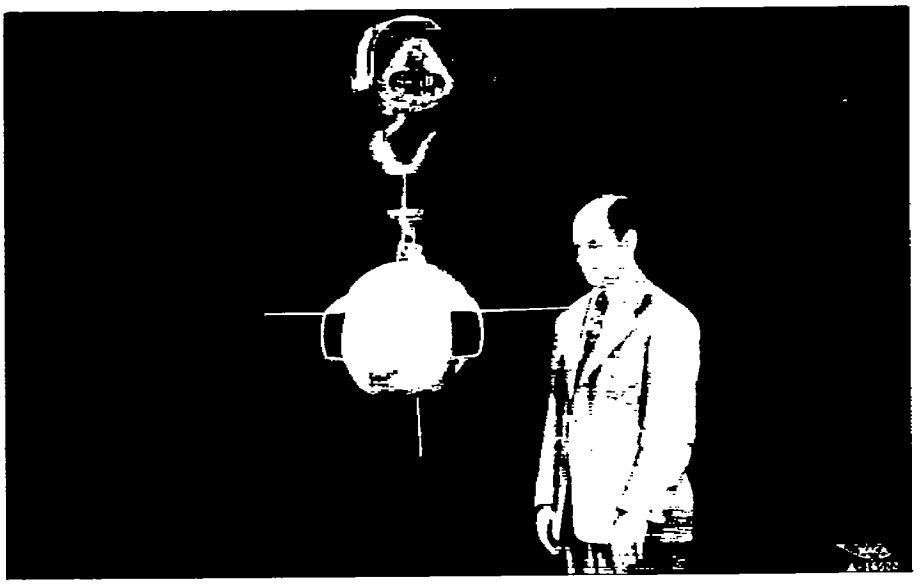

(b) Front view.

Figure 1.- Scoop-inlet model.

[redacted]

Table of Ordinates		
Station, inches	Outside radius, inches	
	R_1	R_2
0	1.19	- -
5.00	1.70	- -
10.00	2.43	- -
15.00	3.21	- -
20.00	3.90	- -
30.00	5.07	- -
40.00	6.02	- -
50.00	6.78	- -
60.00	7.39	- -
70.00	7.87	- -
80.00	8.20	- -
90.00	8.41	- -
100.00	8.49	- -
102.00	8.50	8.50
110.00	8.46	8.50
120.00	8.30	8.50
130.00	8.02	8.50
135.75	7.79	8.50
146.63	7.25	7.55
150.00	7.07	7.25
154.88	6.82	6.82
160.00	6.56	- -
170.00	6.07	- -
180.00	5.59	- -
192.63	4.89	- -
201.63	3.20	- -
211.00	0	- -

Specifications
Horizontal-tail area (incl 1.30 ft² of fus.) 3.45 ft²
Vertical-tail area (incl 1.30 ft² of fus.) 3.45 ft²
Model weight, 1057 lb
Center of gravity sta. 86.25
External wetted area (excluding fins) 8515 in.²

All dimensions are in inches

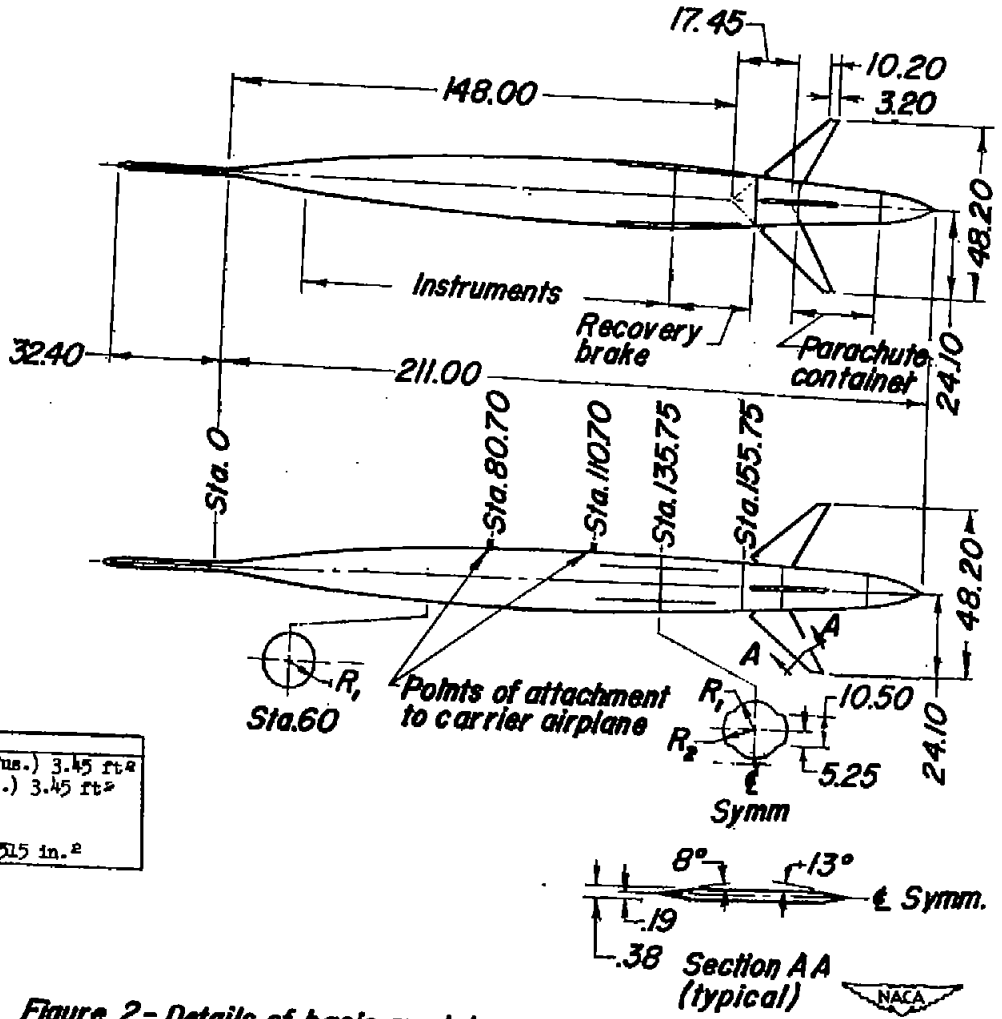

Figure 2 - Details of basic model.

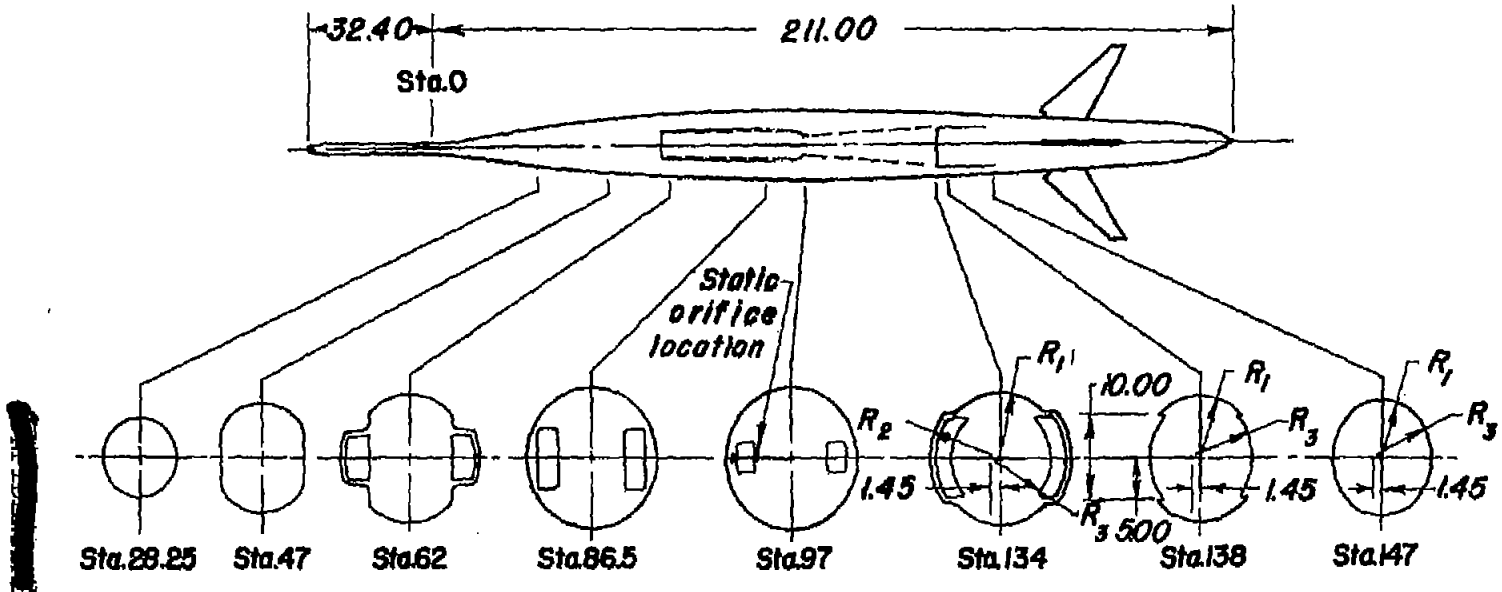

Areas (per duct)	
Entrance	15.80 in.^{2} (L.E. Round Lip)
	13.62 in.^{2} (Sta. 62)
	16.89 in.^{2} (Sta. 86.5)
Entrance to throat	17.34 in.^{2} (Sta. 90)
Outlet	13.75 in.^{2} (Sta. 135.75)

Specifications
Center of gravity, approximately sta. 94
Model weight, approximately 1100 lbs
External wetted area of rounded-lip model (excluding fins) 8571 in.^{2}
External wetted area of sharp-lip model (excluding fins) 8567 in.^{2}

Note

1. All dimensions in inches
2. For ordinates of fuselage see figure 2

Exit dimensions			
Sta.	R_1	R_2	R_3
134.00	7.79	8.50	8.22
138.00	7.68	---	8.22
147.00	7.21	---	8.22

(a) Complete model.

Figure 3.- Details of scoop inlet model.

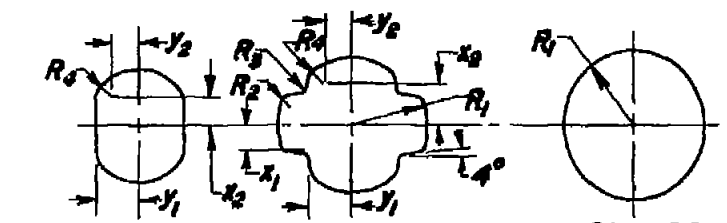

Sta. 28.25 to 60 Sta. 60 to 102 Sta. 102

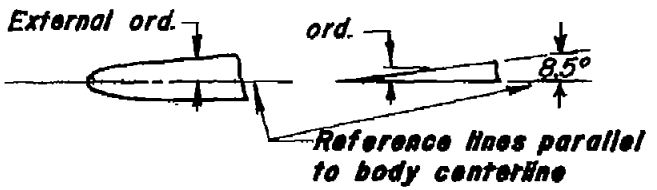

Body dimensions for rounded-lip model								
Body sta.	R_1	R_2	R_3	R_4	x_1	y_1	x_2	y_2
35.0	- - -	- - -	- - -	5.06	- - -	5.37	0.40	0.31
45.0	- - -	- - -	- - -	3.69	- - -	5.37	2.15	1.68
55.0	- - -	- - -	- - -	2.59	- - -	5.37	3.56	2.78
62.0	8.91	0.92	0.50	1.96	3.01	5.47	4.36	3.41
70.0	9.05	.60	1.25	1.86	3.50	5.85	4.46	4.00
80.0	8.91	.50	1.54	3.02	3.87	- - -	3.82	3.52
90.0	8.72	.28	.50	- - -	4.11	- - -	- - -	- - -
102.0	8.50	- - -	- - -	- - -	- - -	- - -	- - -	- - -

Body dimensions for sharp-lip model								
Body sta.	R_1	R_2	R_3	R_4	x_1	y_1	x_2	y_2
35.0	- - -	- - -	- - -	5.06	- - -	5.37	0.40	0.31
45.0	- - -	- - -	- - -	3.69	- - -	5.37	2.15	1.68
55.0	- - -	- - -	- - -	2.59	- - -	5.37	3.56	2.78
62.0	8.59	0.60	0.50	1.96	2.69	5.47	4.36	3.41
70.0	8.99	.60	1.32	1.79	3.41	5.85	4.54	4.06
80.0	8.91	.50	1.54	3.02	3.87	- - -	3.82	3.52
90.0	8.72	.28	.50	- - -	4.11	- - -	- - -	- - -
102.0	8.50	- - -	- - -	- - -	- - -	- - -	- - -	- - -

Rounded-lip ordinates		
Sta.	External ord.	Internal ord.
60.00	0	0
60.10	.119	.101
60.20	.165	.141
60.50	.217	.195
60.75	.245	.203
61.00	.265	.203
61.50	.303	.203
62.00	.338	.203
L.E.R. = 0.078		

Sharp-lip ordinates	
Sta.	Ordinate
60.00	0
60.50	.075
61.00	.130
61.50	.180
62.00	.220
L.E.R. = 0.006	

Note

All dimensions given in inches

(b) Scoop inlet details.

Figure 3. — Continued.

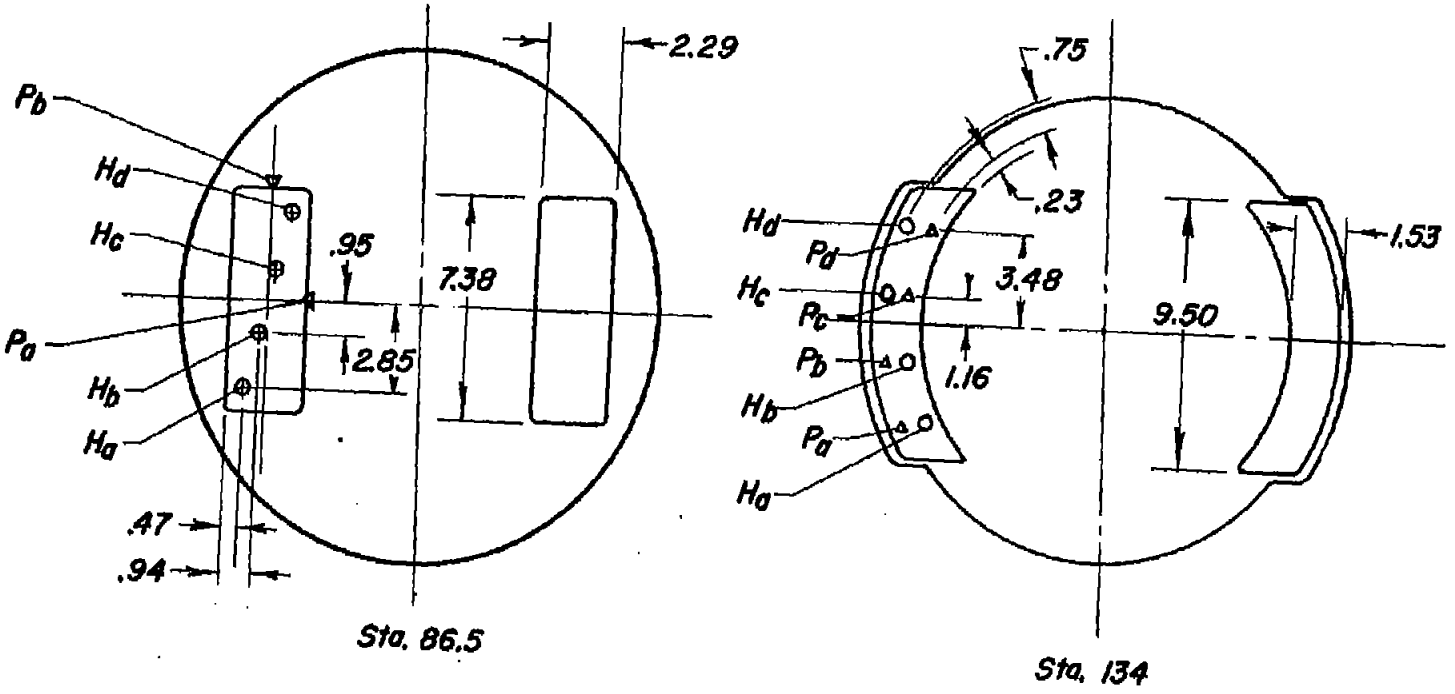

Note
1. H— Total pressure probes
2. P— Static pressure probes
3. All dimensions are in inches

NACA

(c) Location of pressure probes and orifices at stations 86.5 and 134.
Figure 3. – Continued.

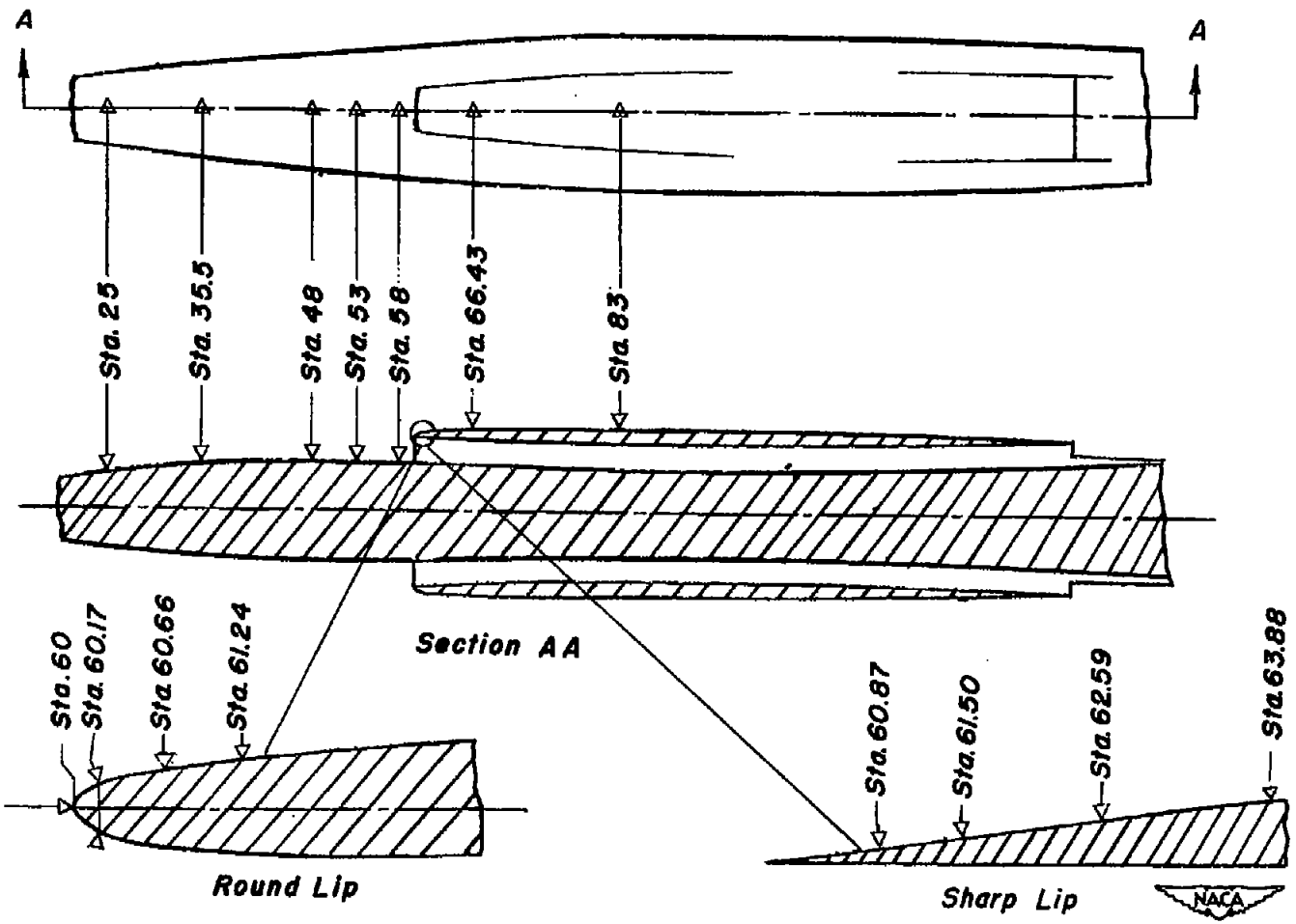

(d) Orifice locations

Figure 3. – Concluded.

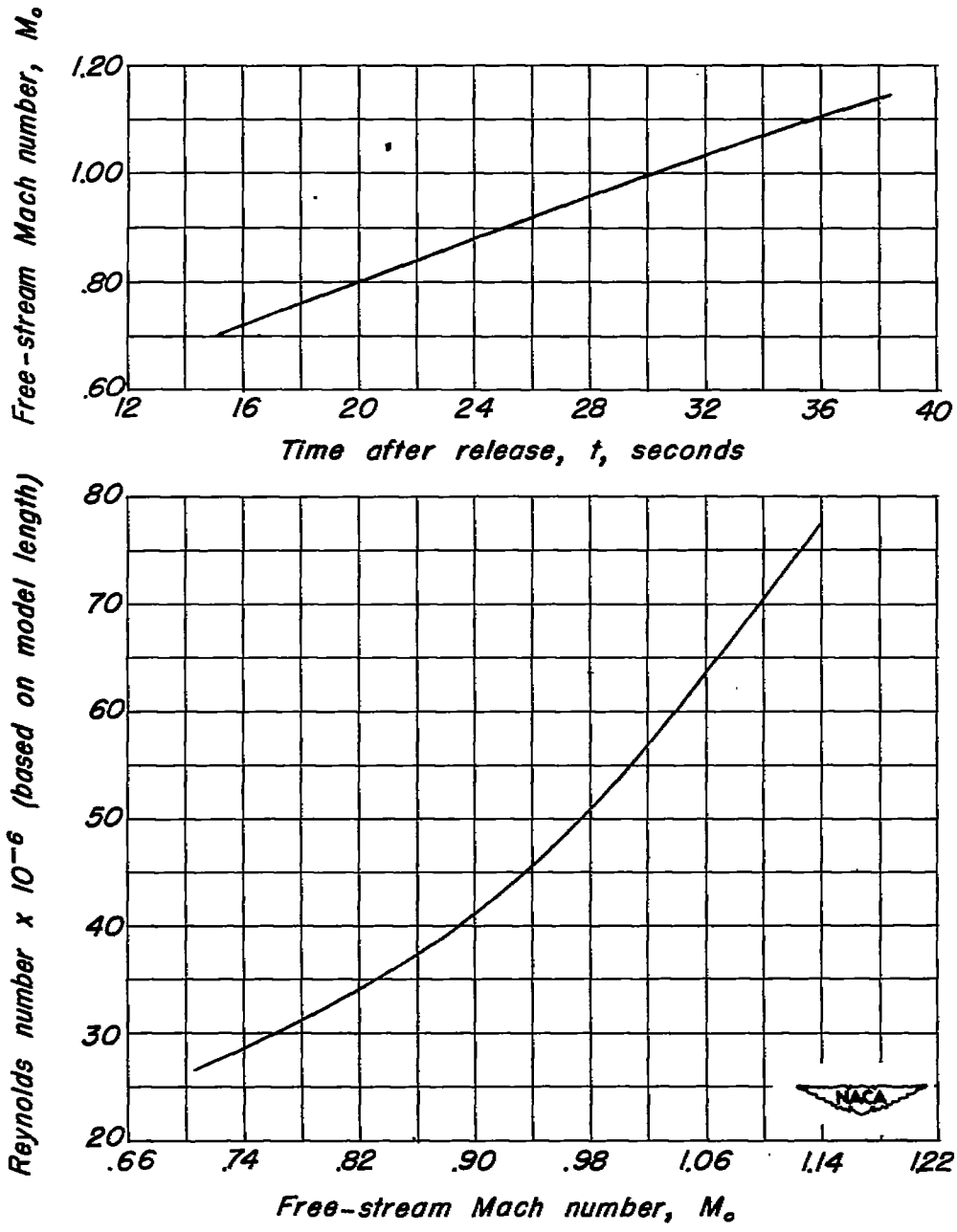

Figure 4.- Typical variation of Mach number with time and Reynolds number with Mach number during free fall of model.

[redacted]

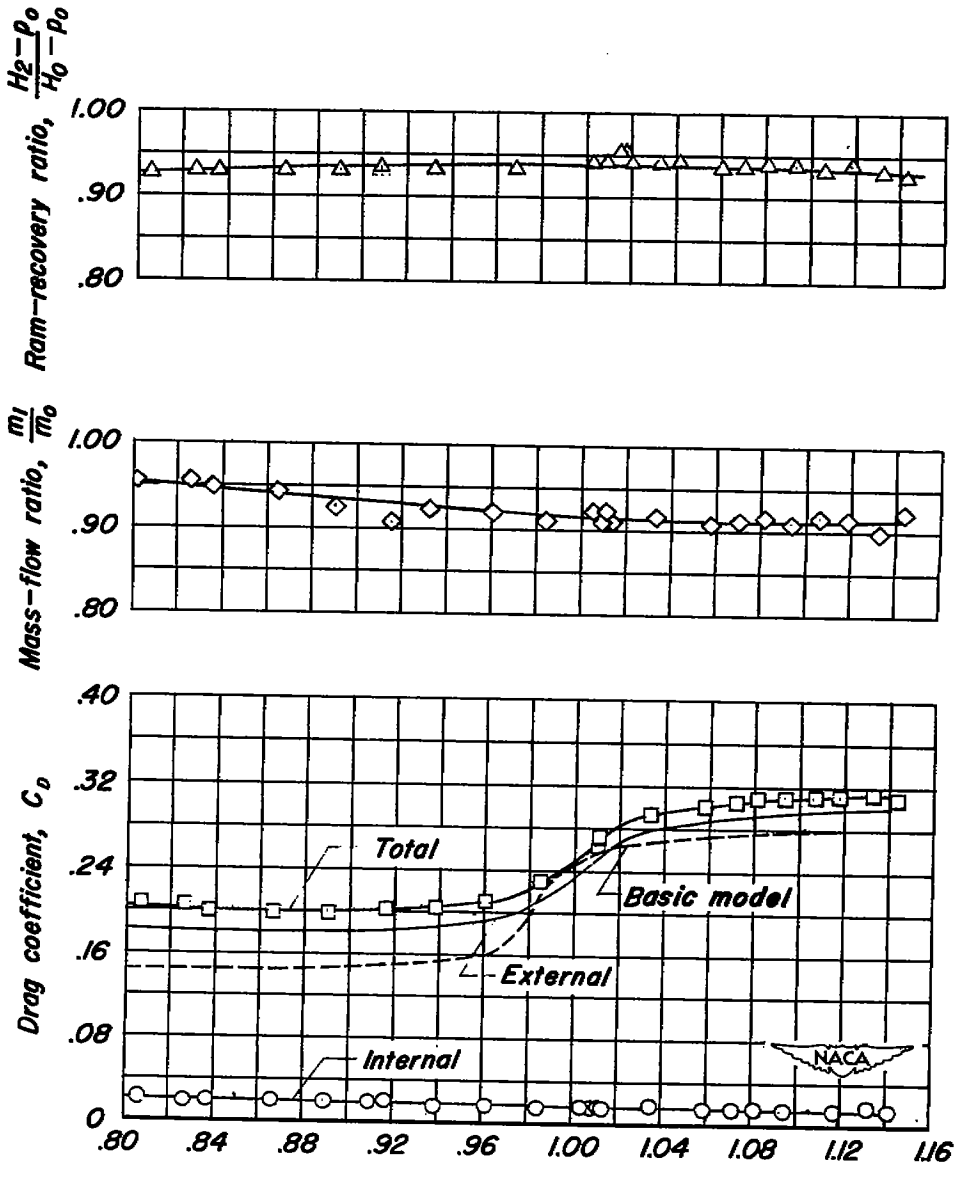

(a) $\frac{A_3}{A_1} = 1.00$

Figure 5. – Variations of drag coefficients, pressure recovery, and mass-flow ratio with free-stream Mach number for scoop inlet with rounded lips.

[redacted]

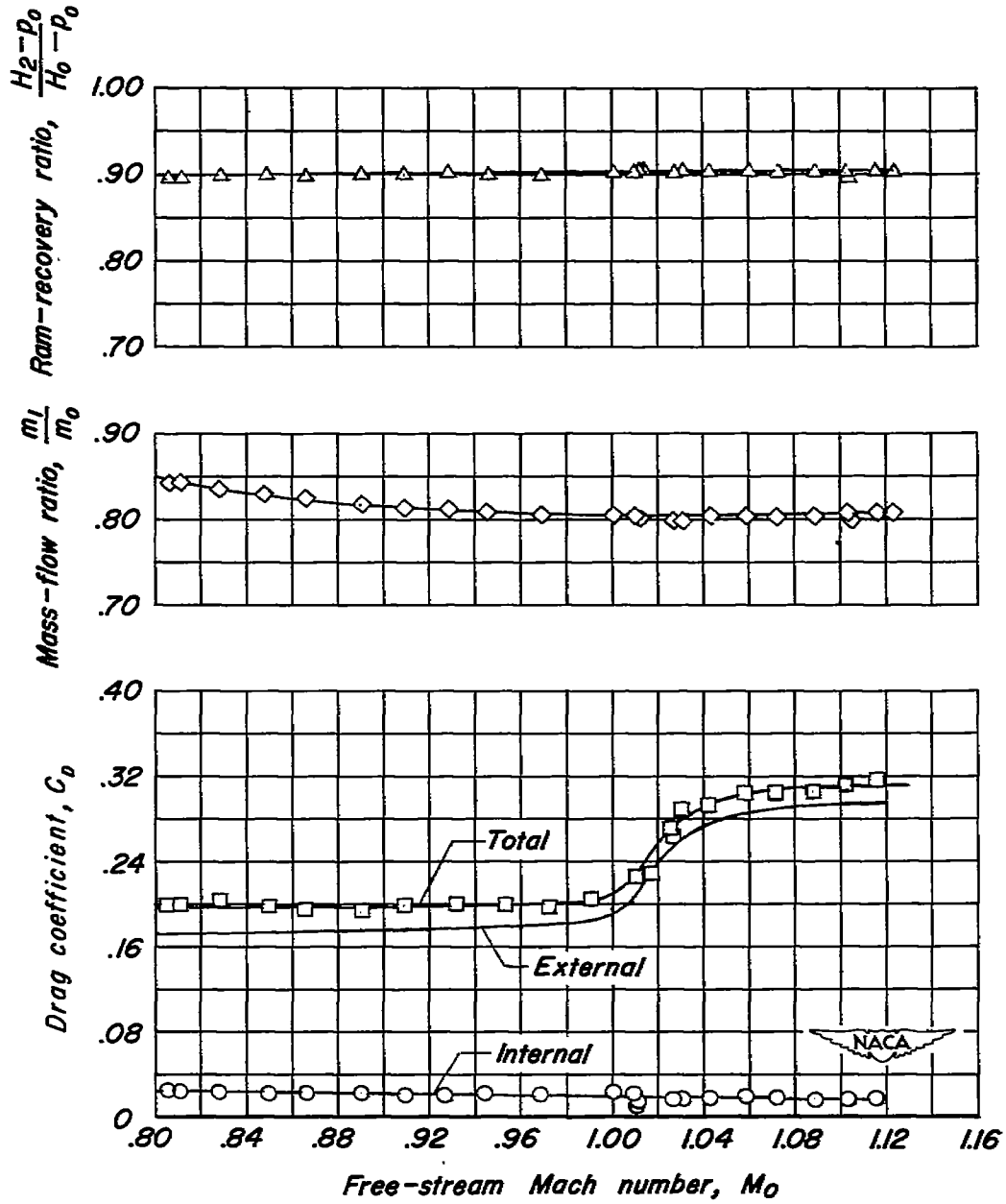

(b) $\frac{A_3}{A_1} = 0.889$

Figure 5.- Continued.

[redacted]

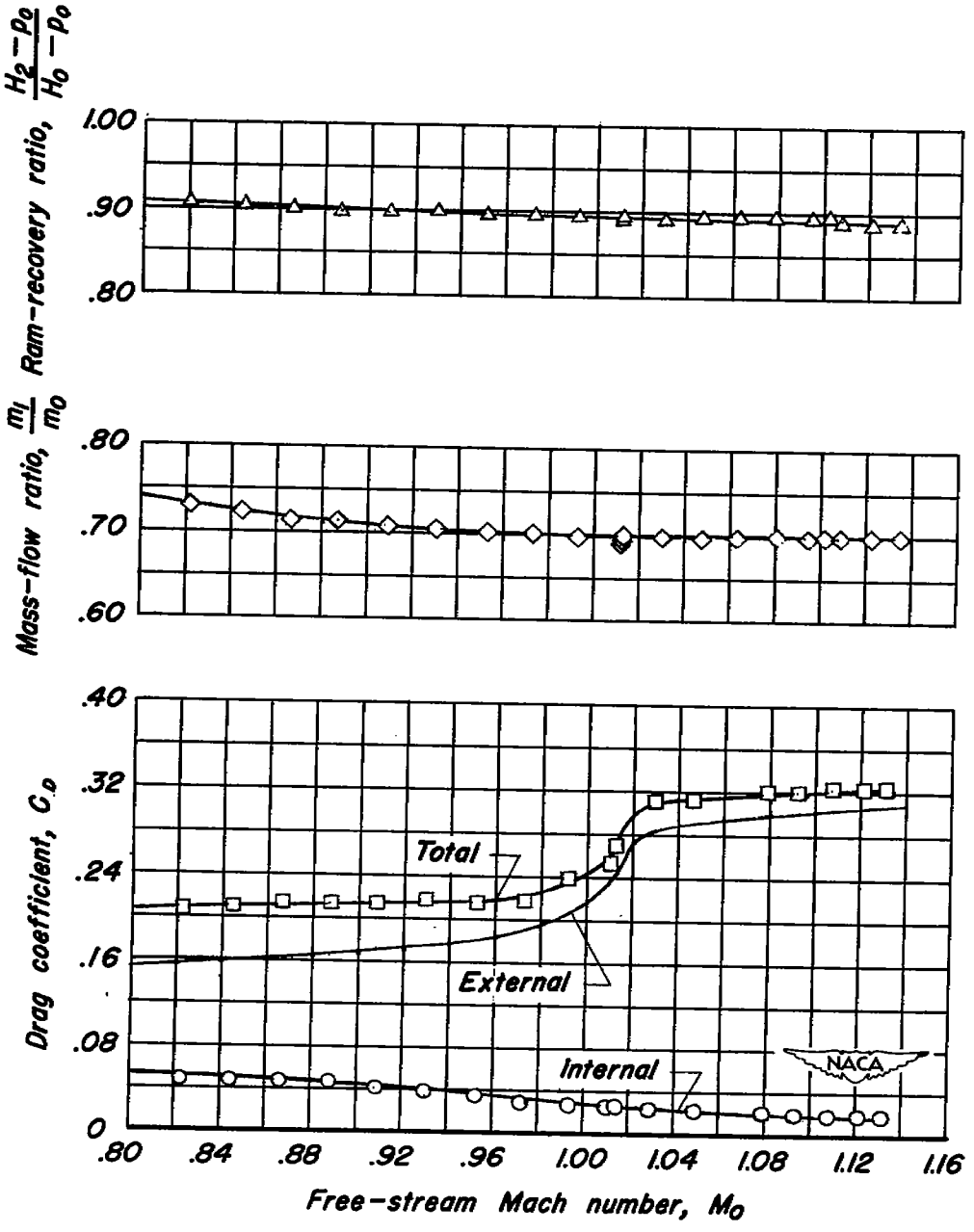

(c) $\frac{A_3}{A_1} = 0.777$

Figure 5. – Continued.

[redacted]

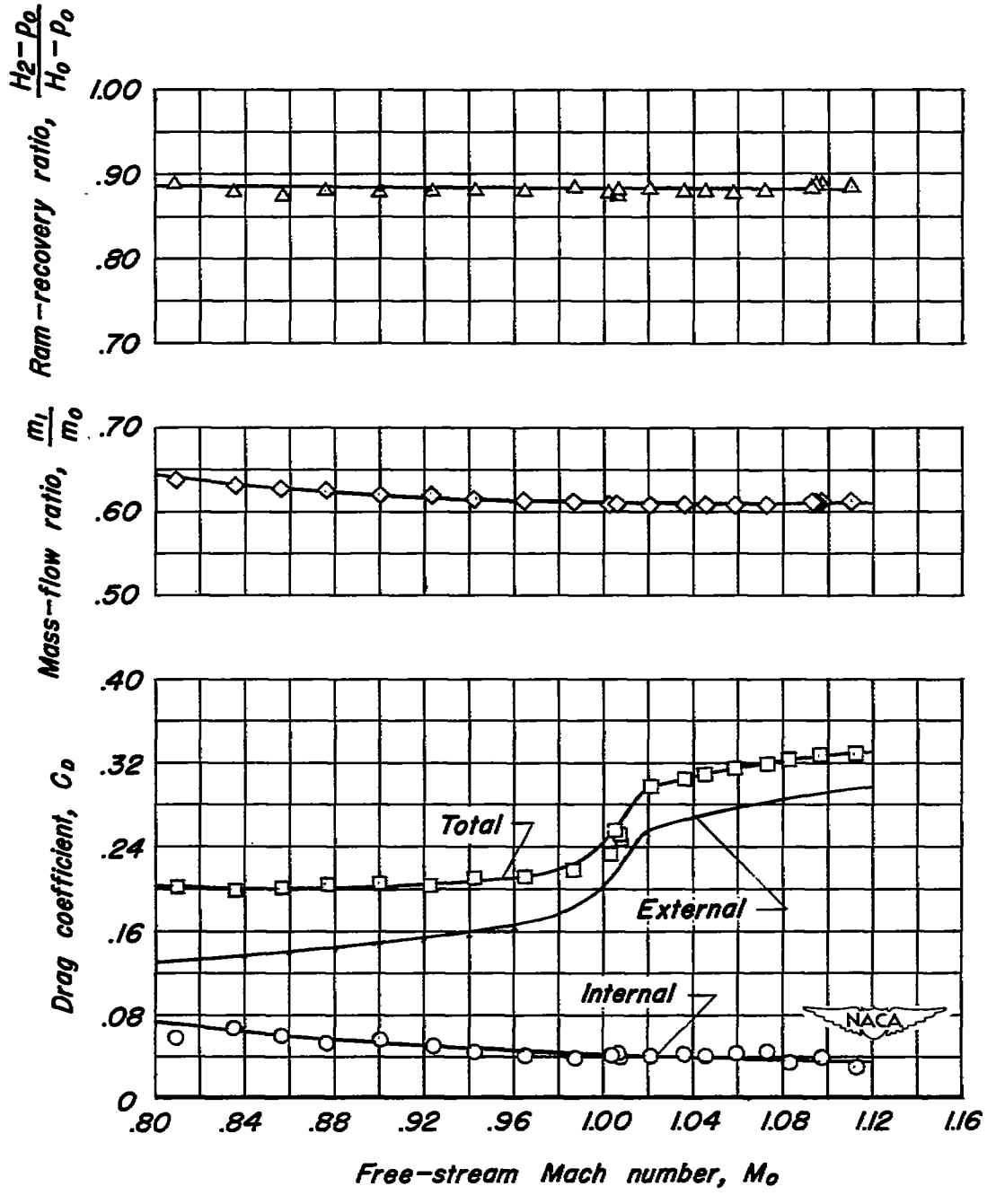

(d) $\frac{A_3}{A_1} = 0.683$

Figure 5.- Concluded.

[redacted]

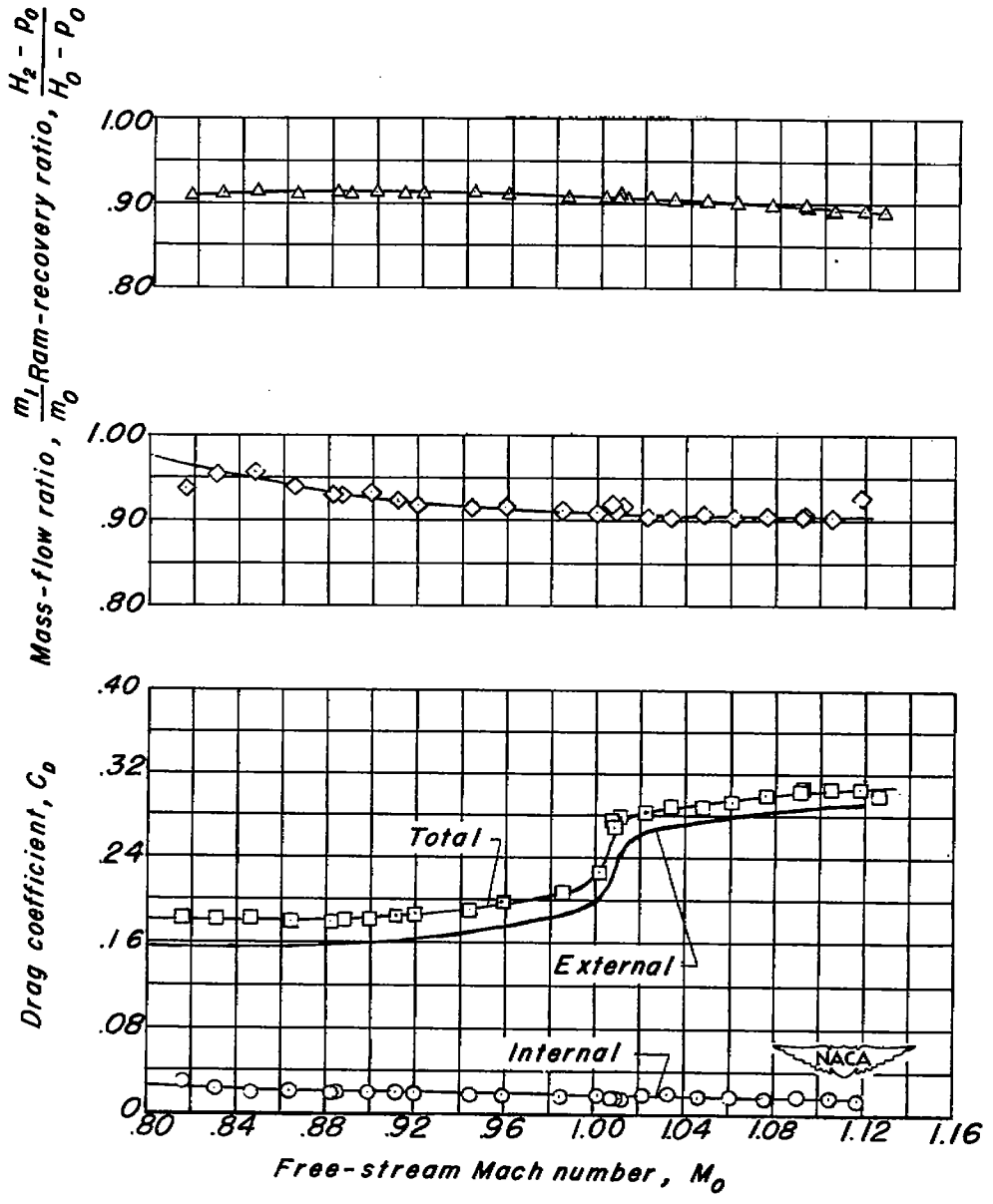

(a) $\frac{A_3}{A_1} = 1.00$

Figure 6.—Variation of drag coefficients, pressure recovery, and mass-flow ratio with free-stream Mach number for scoop inlet with sharp lip.

[redacted]

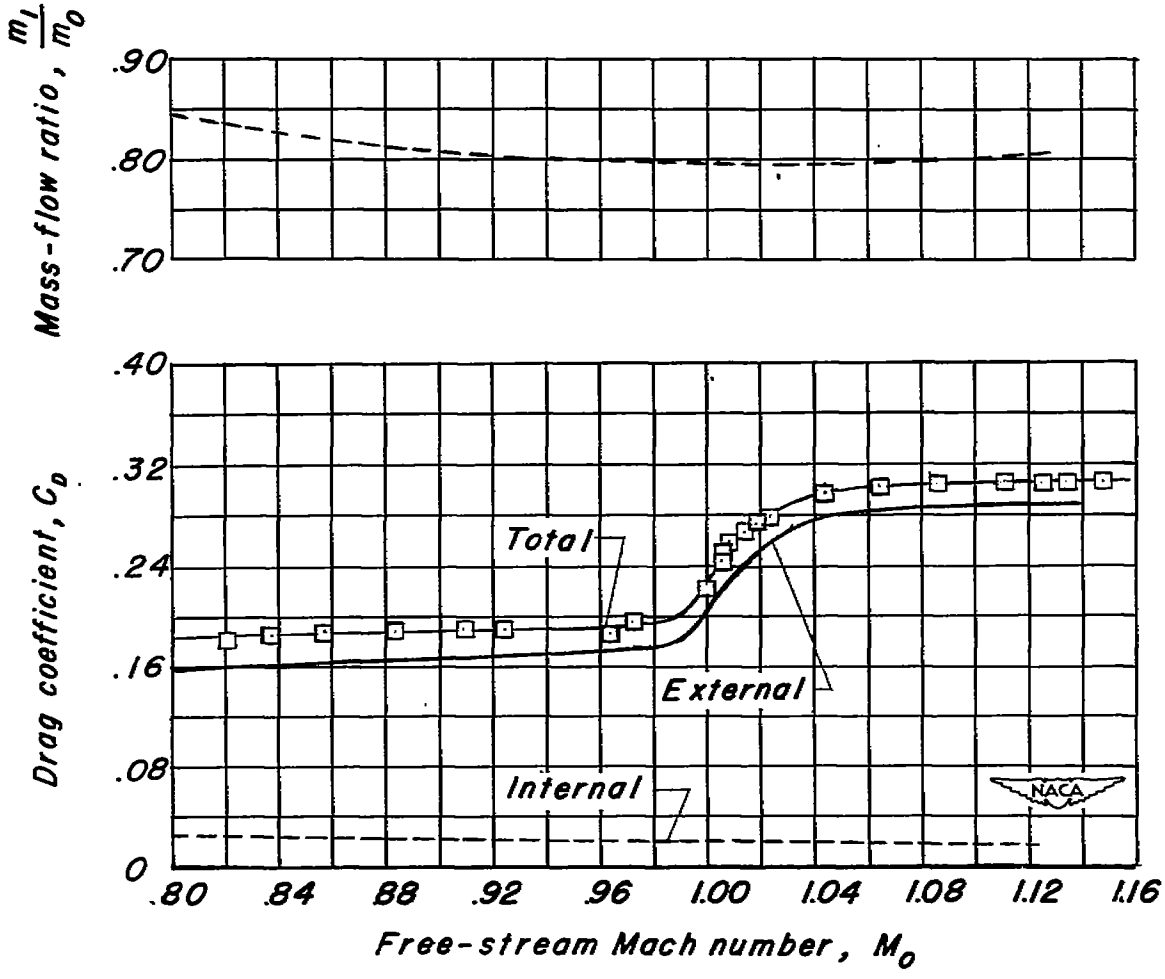

(b) $\frac{A_3}{A_1} = 0.889$

Figure 6.– Continued.

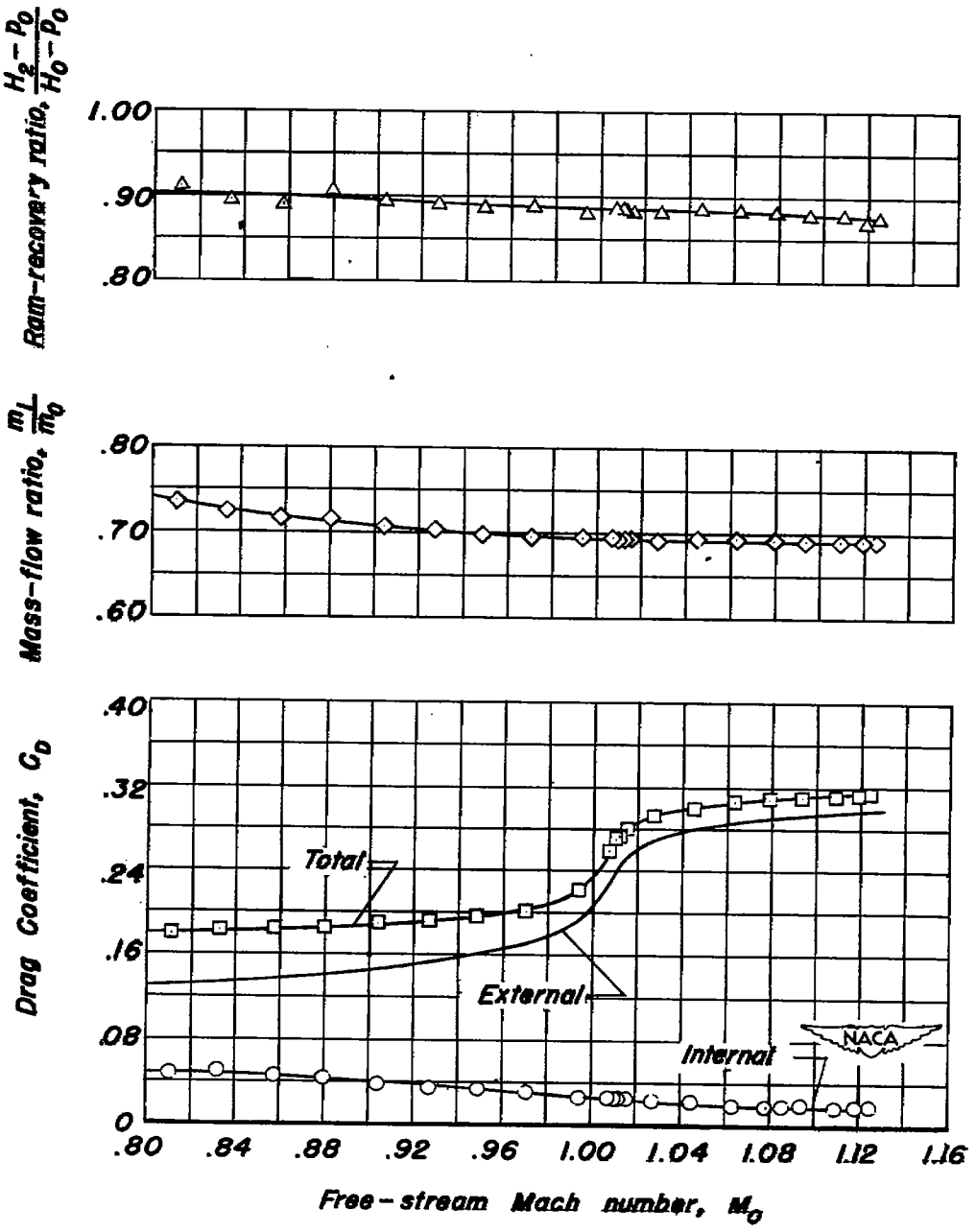

(c) $\frac{A_3}{A_1} = 0.777$

Figure 6.—Concluded.

[redacted]

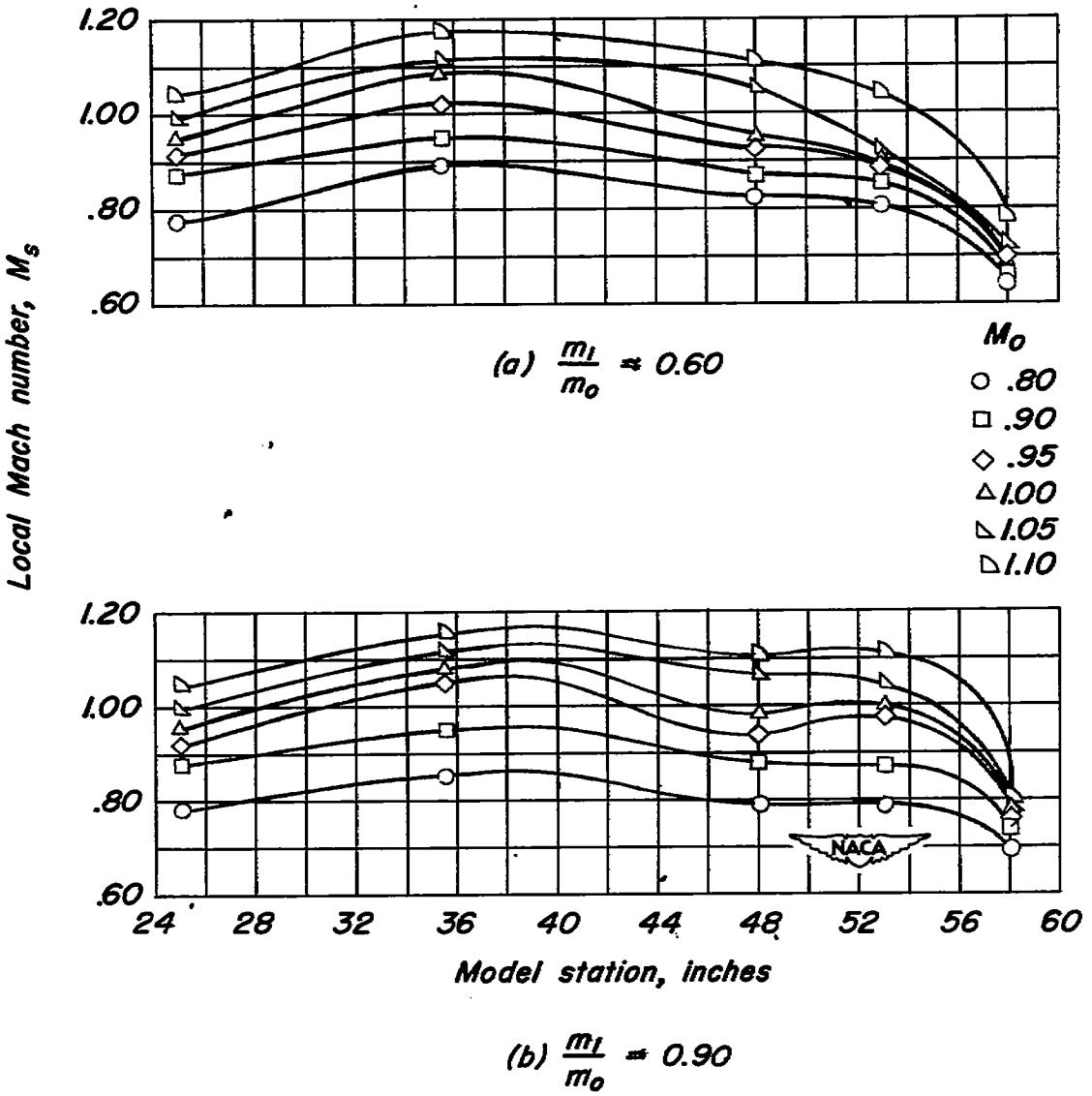

Figure 7. — Mach number distribution along model surface forward of the scoop inlet with a rounded lip at mass-flow ratios of about 0.60 and 0.90.

[redacted]

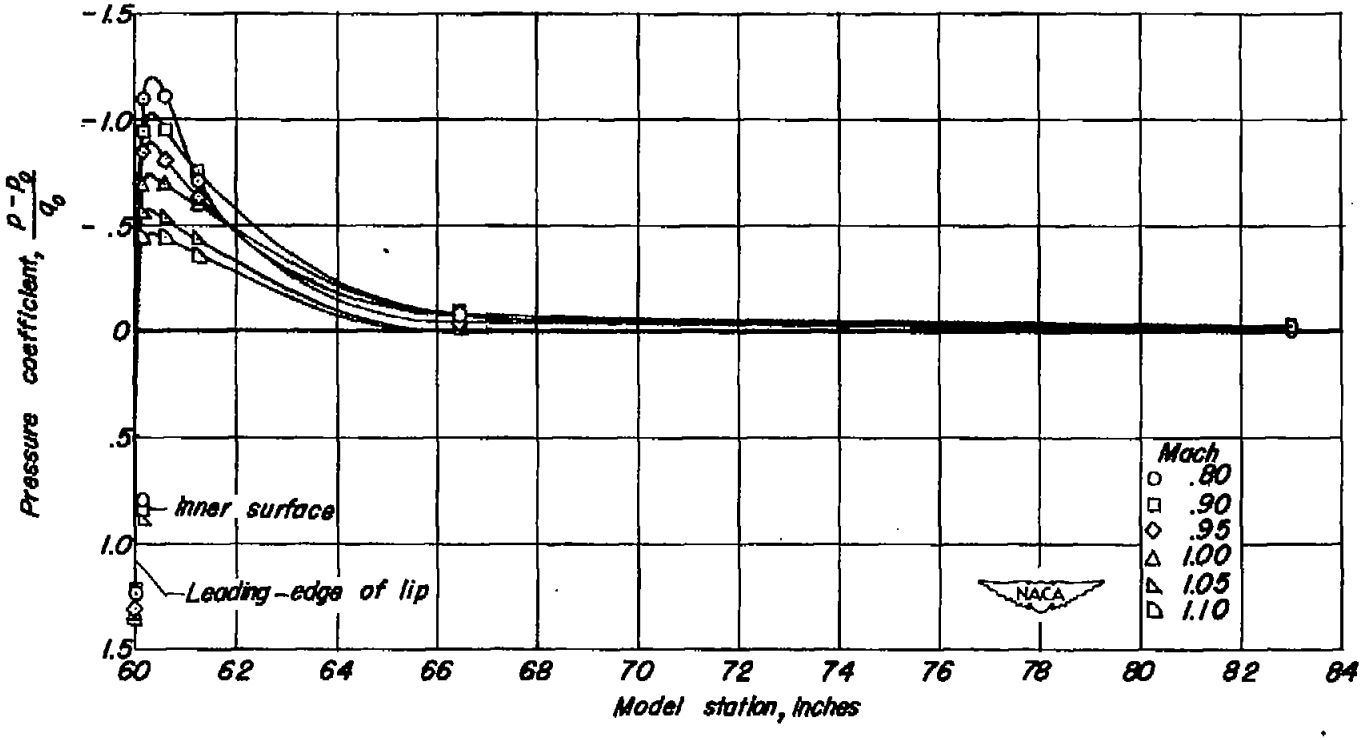

(a) Mass-flow ratio, $\frac{m_1}{m_0} = 0.60$

Figure 8.- Variation of pressure coefficient along the center line of the rounded lip with distance behind the lip leading-edge at mass-flow ratios of about 0.60 and 0.90.

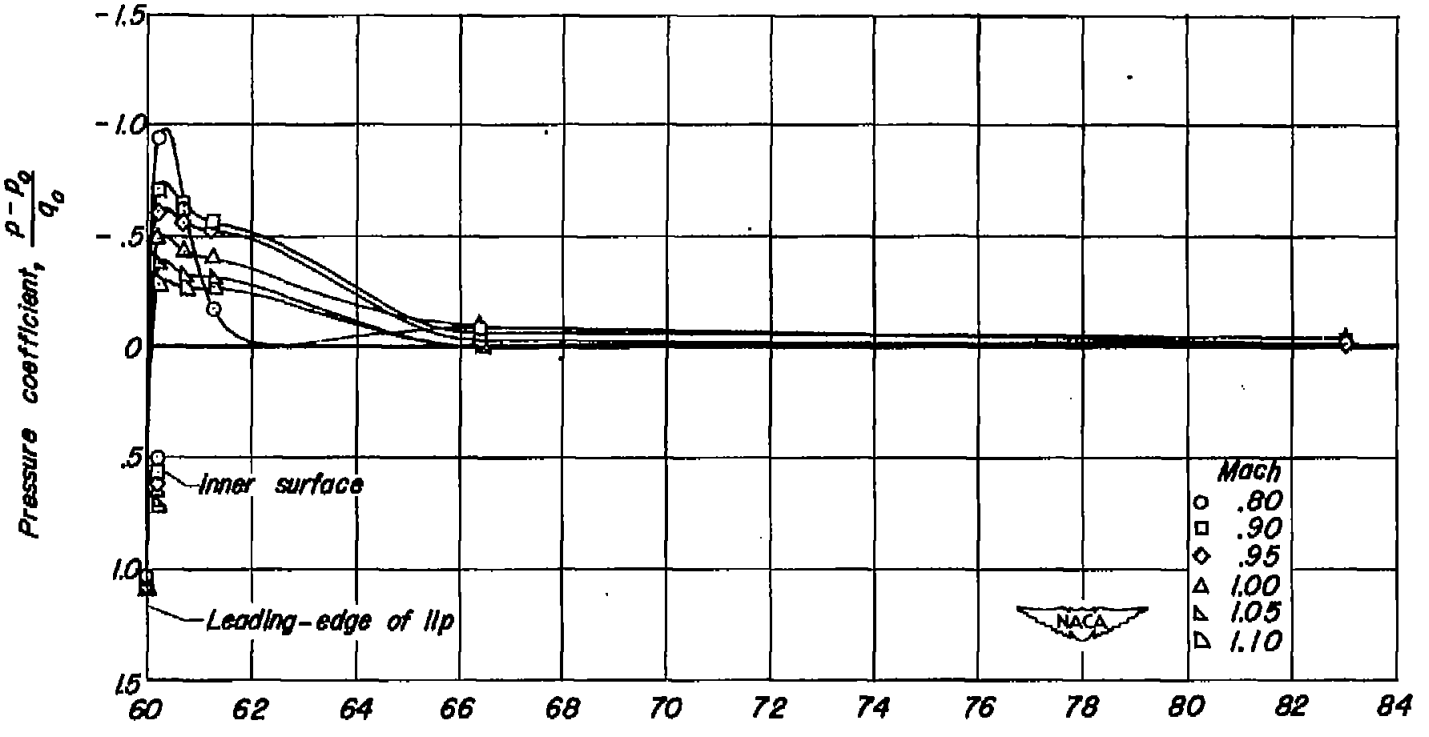

(b) Mass-flow ratio, $\frac{m_1}{m_0} \approx 0.90$

Figure 8.- Concluded.

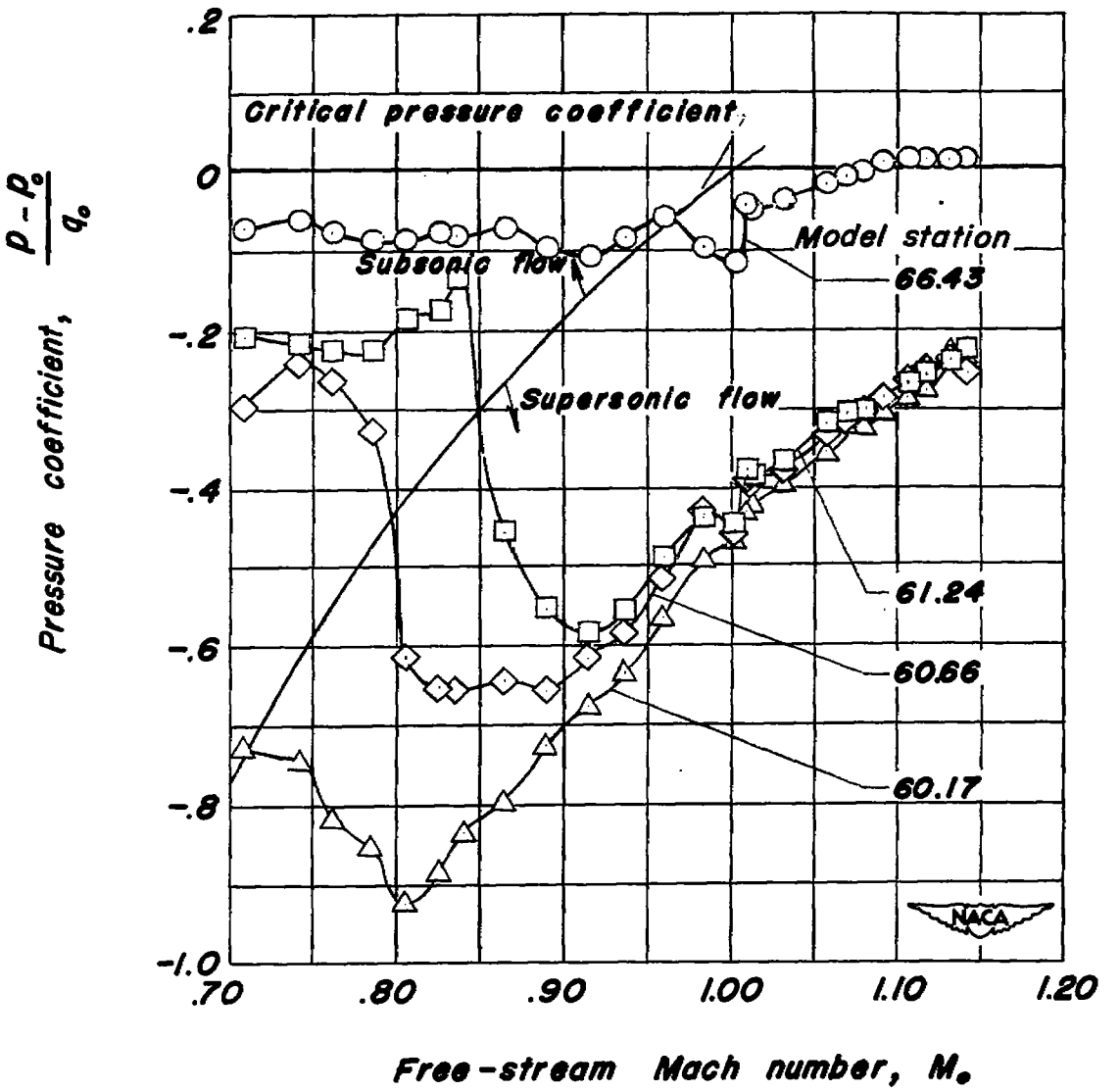

Figure 9.- Variation of lip pressure coefficients along center line of outer surface of the rounded lip with free-stream Mach number at a mass-flow ratio of about 0.90.

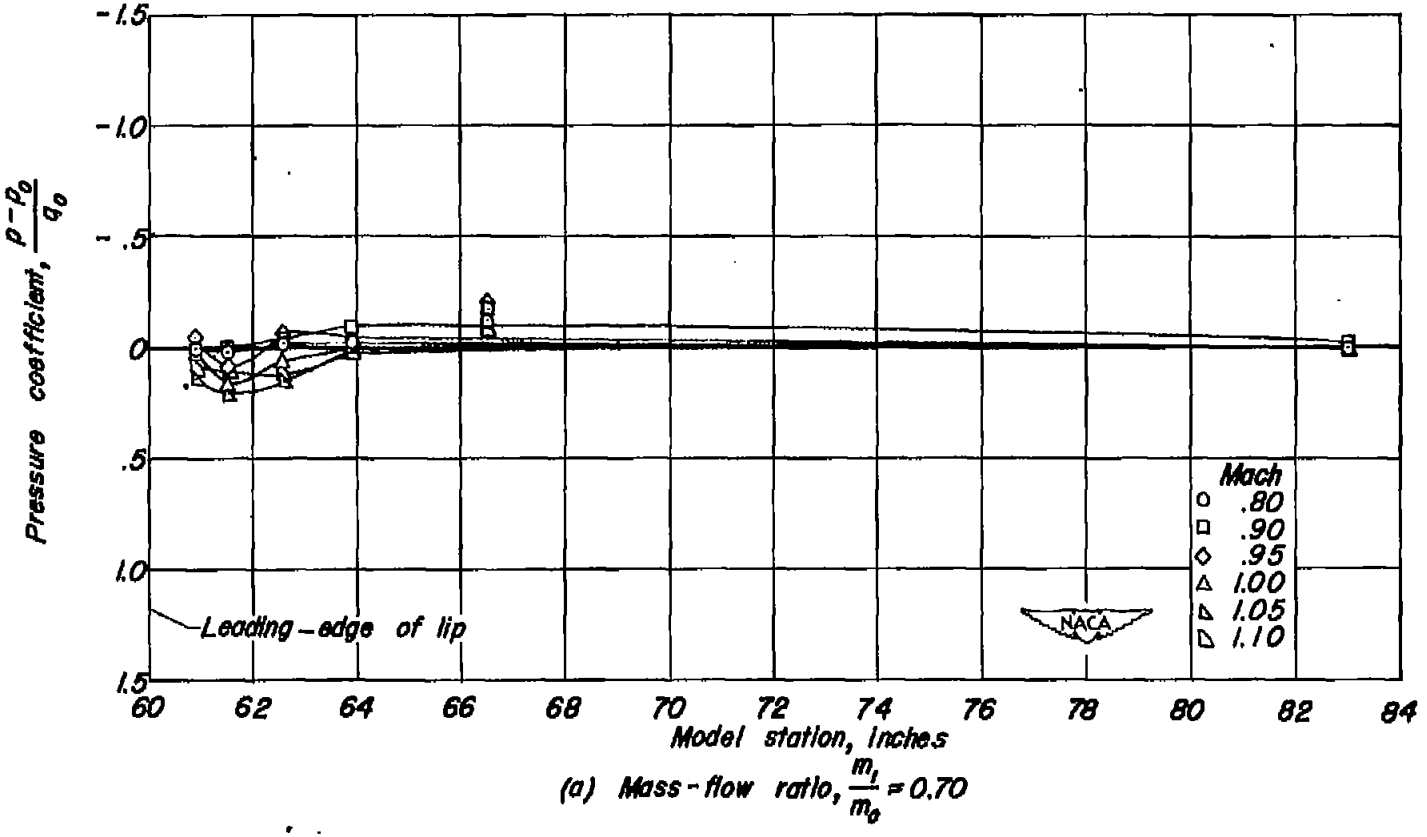

(a) Mass-flow ratio, $\frac{m_1}{m_o} = 0.70$

Figure 10.- Variation of pressure coefficient along center line of sharp lip with distance behind lip leading-edge at mass-flow ratios of about 0.70 and 0.90.

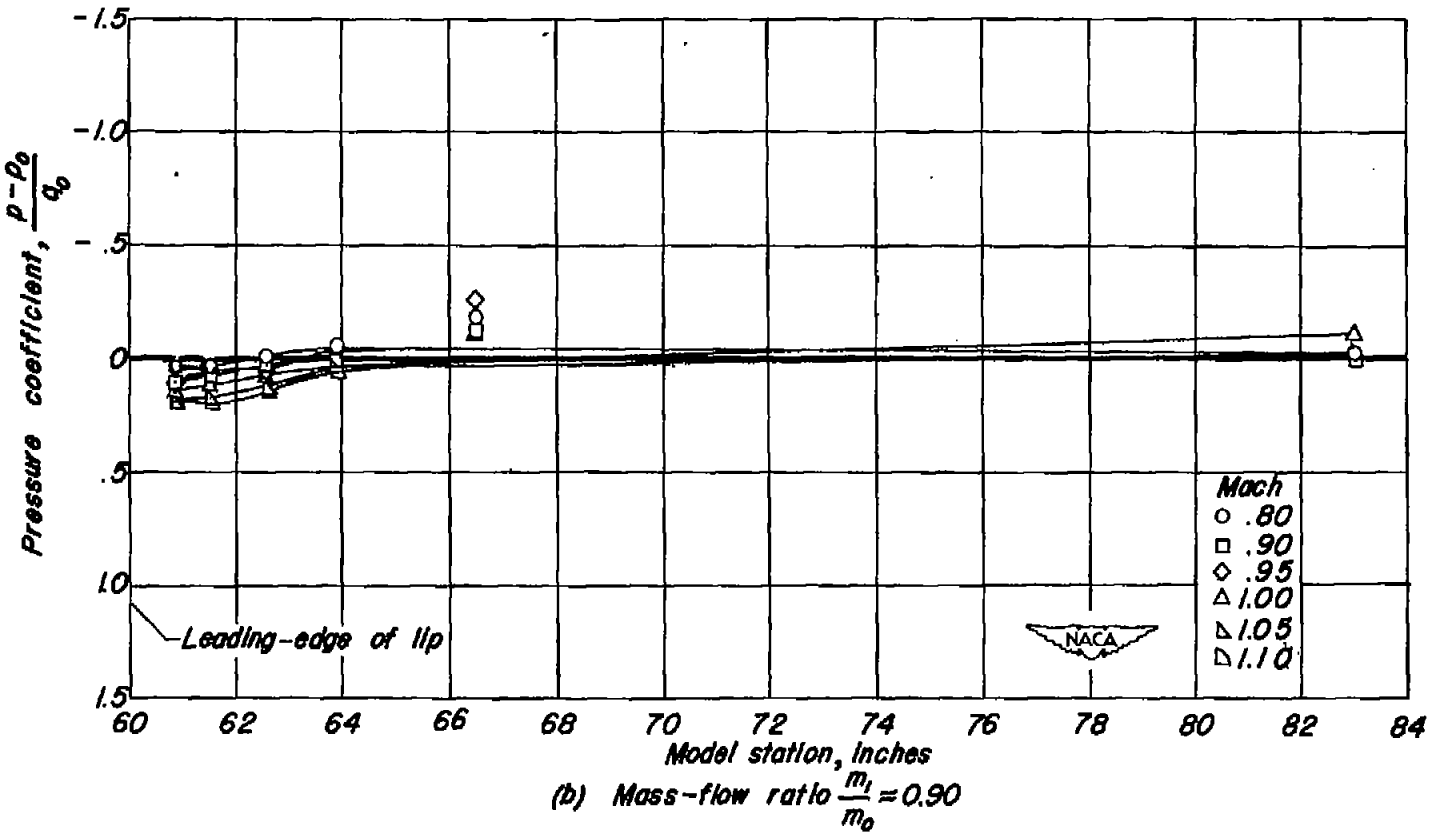

(b) Mass-flow ratio $\frac{m_1}{m_0} = 0.90$

Figure 10.- Concluded.

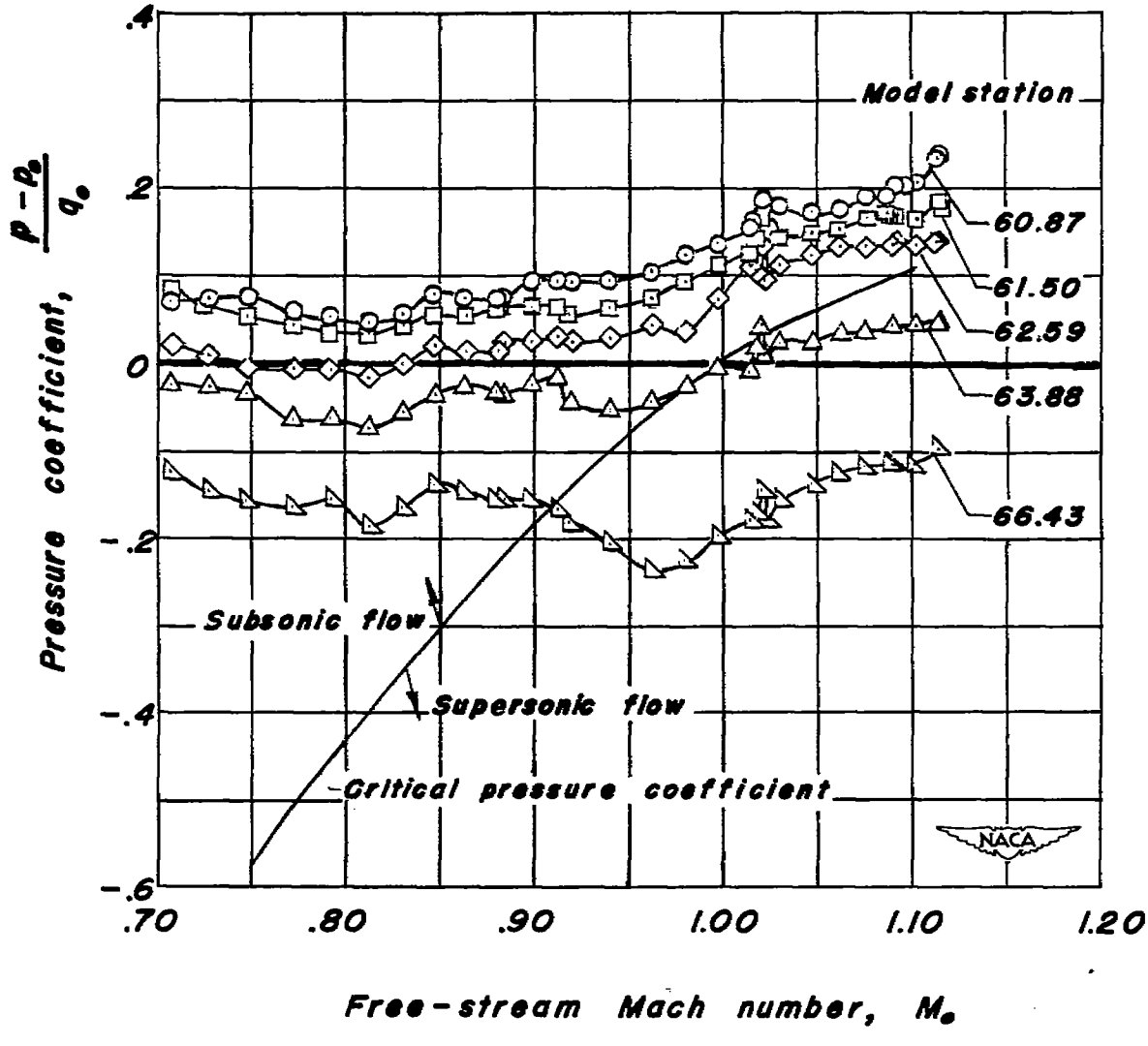

Figure 11.—Variation of lip pressure coefficients along center line of outer surface of the sharp lip with free-stream Mach number at a mass-flow ratio of about 0.90.

[redacted]

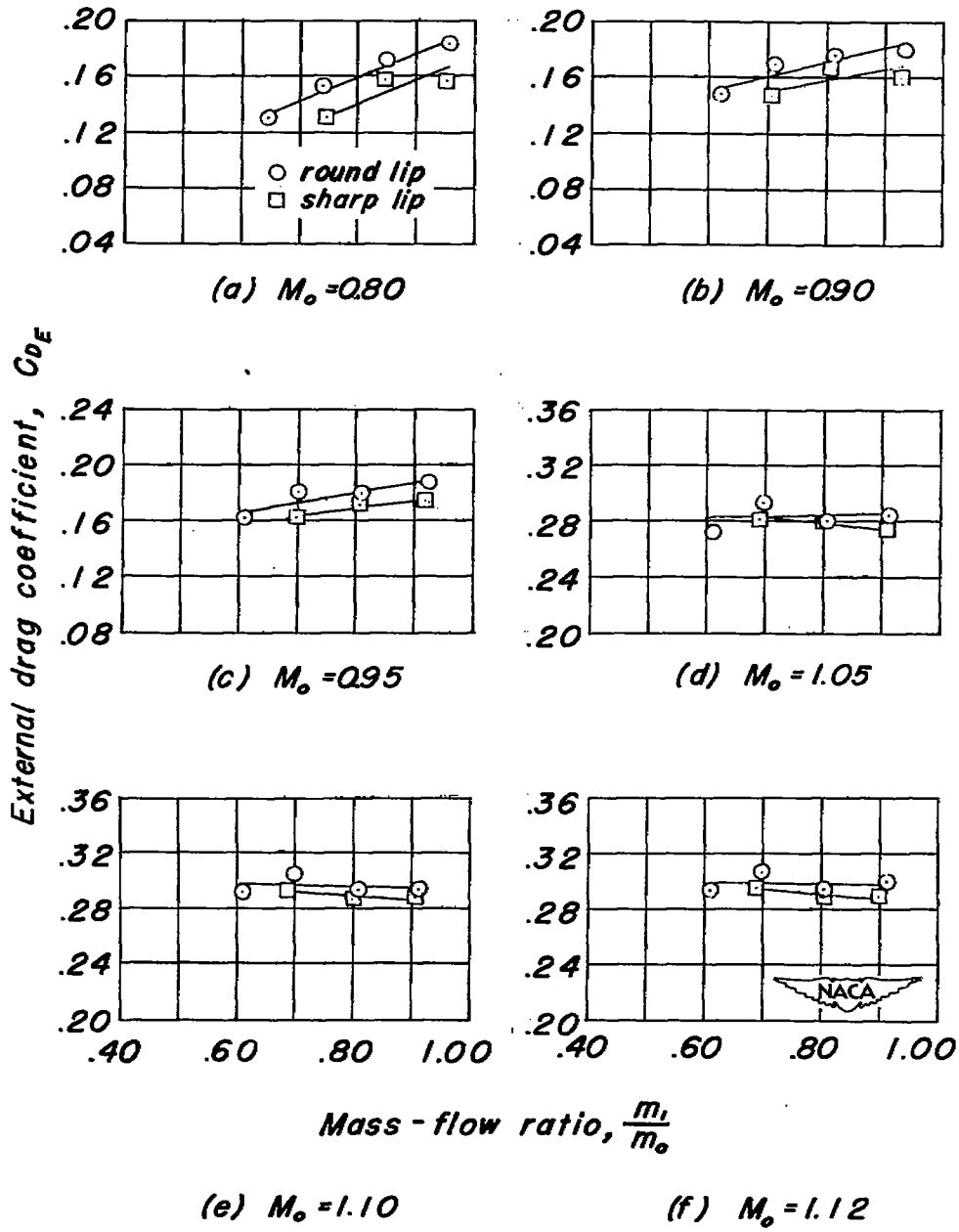

Figure 12. — Variation of external drag coefficient with mass-flow ratio for the scoop-inlet model with rounded and sharp lips at various Mach numbers.

[redacted]

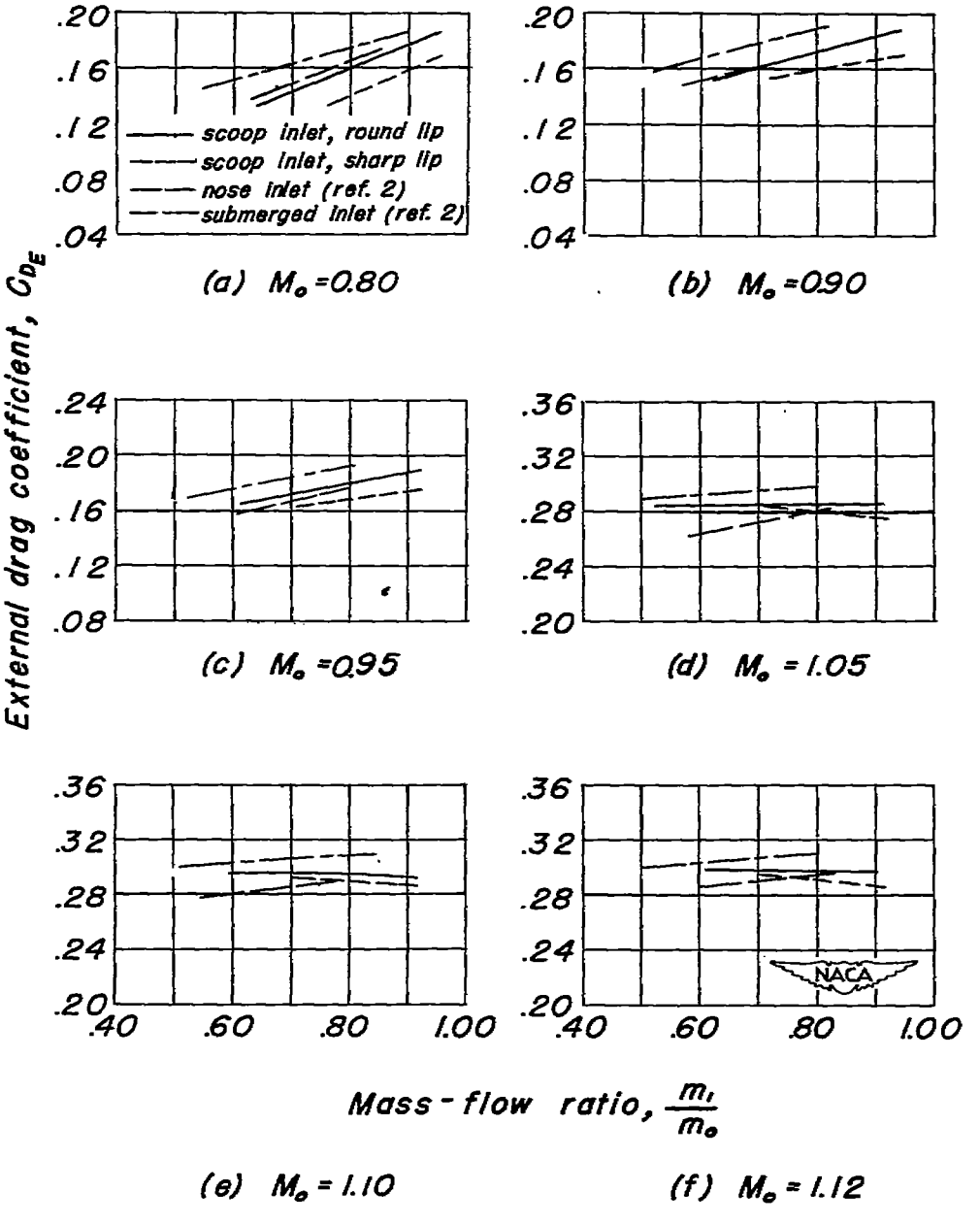

Figure 13.— Comparison of variation of external drag coefficient with mass-flow ratio of scoop inlet with that for submerged inlet and nose inlet.

[redacted]

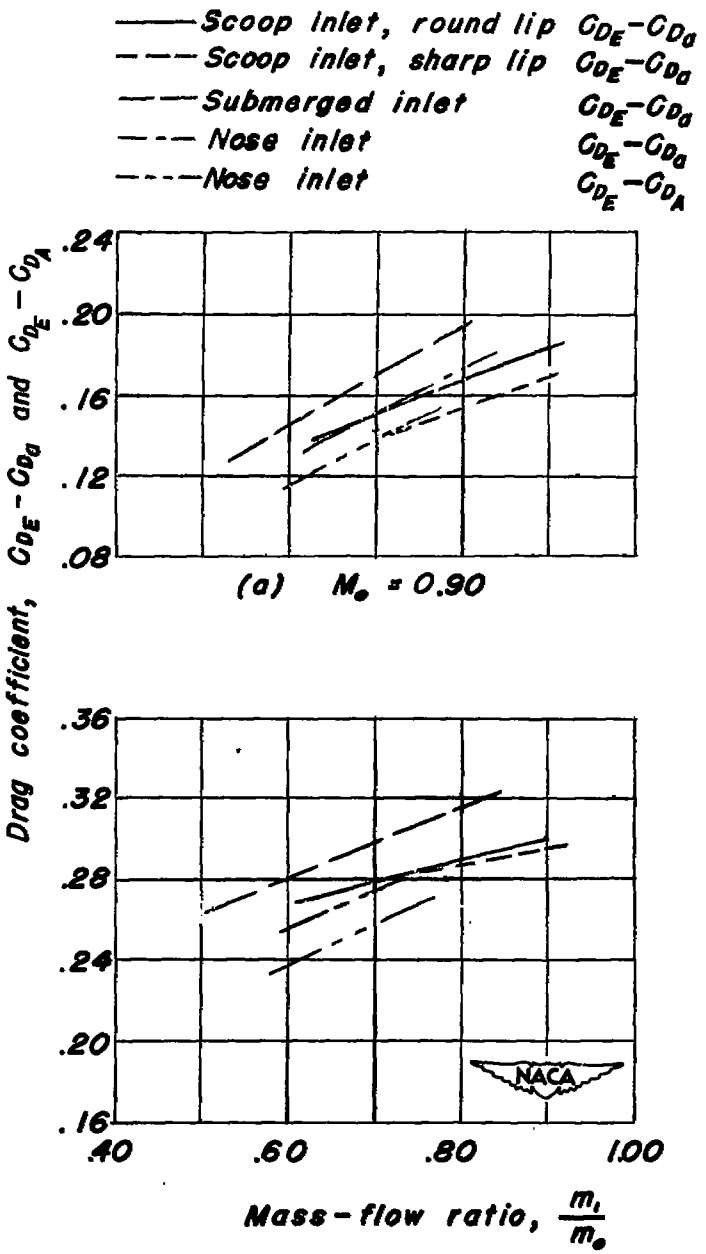

Figure 14.– Variation with mass-flow ratio of external-drag less computed inlet incremental-drag for all inlet models and external drag less additive-drag for nose-inlet model.

[redacted]

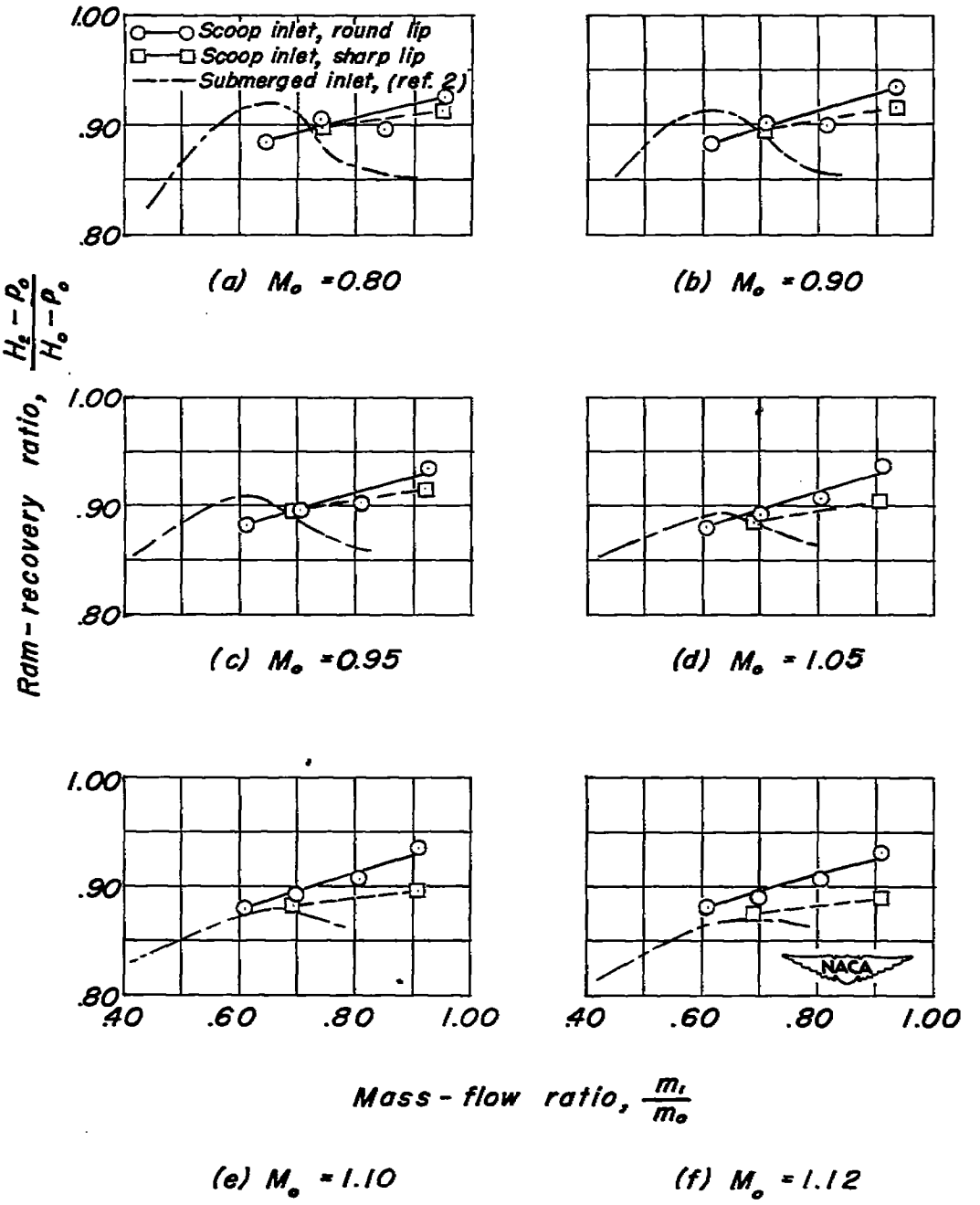

Figure 15.– Variation of ram-recovery ratio of scoop-inlet model with mass-flow ratio at various Mach numbers.

[redacted]

[redacted]

[redacted]